BIOCHEMISTRY
including biophysical chemistry & molecular biology

Article

pubs.acs.org/biochemistry

Strategies for Modulating the pH-Dependent Activity of a Family 11 Glycoside Hydrolase

Martin L. Ludwiczek,[†,‡,§] Igor D'Angelo,[†] Gary N. Yalloway,[†,‡] Jacob A. Brockerman,[†,‡,§] Mark Okon,[†,‡,§] Jens E. Nielsen,[#] Natalie C. J. Strynadka,[†] Stephen G. Withers,[†,‡,∥] and Lawrence P. McIntosh*[,†,‡,§]

[†]Department of Biochemistry and Molecular Biology, University of British Columbia, Vancouver, British Columbia, Canada V6T 1Z3

[‡]Department of Chemistry, University of British Columbia, Vancouver, British Columbia, Canada V6T 1Z1

[§]Michael Smith Laboratories, University of British Columbia, Vancouver, British Columbia, Canada V6T 1Z4

[#]School of Biomolecular and Biomedical Science, Centre for Synthesis and Chemical Biology, UCD Conway Institute, University College Dublin, Belfield, Dublin 4, Ireland

[∥]Centre for High-throughput Biology, University of British Columbia, Vancouver, British Columbia, Canada V6T 1Z4

Supporting Information

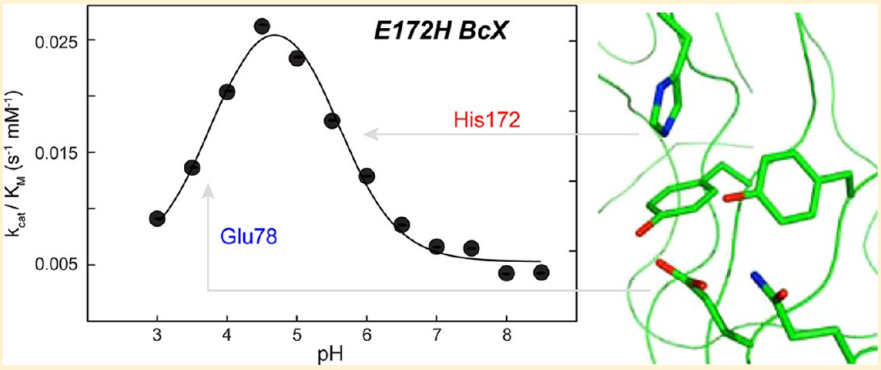

ABSTRACT: The pH-dependent activity of wild-type *Bacillus circulans* xylanase (BcX) is set by the pK_a values of its nucleophile Glu78 and general acid/base Glu172. Herein, we examined several strategies to manipulate these pK_a values and thereby shift the pH_{opt} at which BcX is optimally active. Altering the global charge of BcX through random succinylation had no significant effect. Mutation of residues near or within the active site of BcX, but not directly contacting the catalytic carboxyls, either had little effect or reduced its pH_{opt}, primarily by lowering the apparent pK_a value of Glu78. However, mutations causing the largest pK_a changes also impaired activity. Although not found as a general acid/base in naturally occurring xylanases, substitution of Glu172 with a His lowered the pH_{opt} of BcX from 5.6 to 4.7 while retaining 8% activity toward a xylobioside substrate. Mutation of Asn35, which contacts Glu172, to either His or Glu also led to a reduction in pH_{opt} by ∼1.2 units. Detailed pK_a measurements by NMR spectroscopy revealed that, despite the opposite charges of the introduced residues, both the N35H and N35E forms of BcX utilize a reverse protonation mechanism. In this mechanism, the pK_a value of the general acid is lower than that of the nucleophile, and only a small population of enzyme is in a catalytically competent ionization state. However, overall activity is maintained due to the increased strength of the general acid. This study illustrates several routes for altering the pH-dependent properties of xylanases, while also providing valuable insights into complex protein electrostatics.

Glycoside hydrolases (GHs) catalyze the hydrolysis of carbohydrates and thus play critical roles in biology and have many practical applications in medicine and biotechnology. GHs typically exploit two catalytic carboxyls/carboxylates to cleave a glycosidic linkage with either net retention or inversion of stereochemistry.[1,2] In the inverting mechanism, hydrolysis occurs via a single S_N2 step with general base catalyzed attack of water at the sugar anomeric center, coupled with general acid assistance of aglycone departure. In the retaining mechanism, a double-displacement pathway is followed with direct nucleophilic attack of one carboxylate on the glycone to produce a covalent glycosyl-enzyme intermediate. The partner carboxyl serves a dual role of general acid during the glycosylation step to catalyze aglycone departure, and then general base during deglycosylation to activate a nucleophilic water. With rate enhancements of up to 10^{17}-fold, GHs are among the most proficient known enzymes, and thus understanding the structural, dynamic, and electrostatic bases underlying these two mechanisms remains the subject of considerable scientific effort.[3,4]

Received: January 8, 2013
Revised: April 9, 2013
Published: April 12, 2013

Bacillus circulans xylanase (BcX) is a 20 kDa family GH-11 retaining endo-β-(1,4)-xylanase that has been characterized in great detail by kinetic, X-ray crystallographic, and NMR spectroscopic methods.[5−9] In particular, the bell-shaped pH-dependent k_{cat}/K_m activity profile of this model GH can be explained by the NMR-measured pK_a values of its catalytic residues (Scheme 1).[10] At pH_{opt} 5.7, where BcX is optimally

Scheme 1

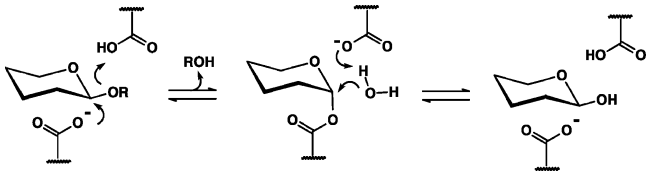

active, Glu78 (pK_a = 4.6) is predominantly deprotonated to serve as a nucleophile for the rate-limiting glycosylation step, whereas Glu172 (pK_a = 6.7) is protonated to act as a general acid. Subsequently, the pK_a value of Glu172 drops to 4.2 in a long-lived glycosyl-enzyme intermediate with Glu78 covalently bonded to a 2-deoxy-2-fluoro-β-xylobiosyl moiety (2FXb). The dramatic reduction in the pK_a value of Glu172, which is primarily due to the loss of charge repulsion from Glu78, enables this residue to act as a general base and thereby facilitate deglycosylation. Importantly, the "pK_a cycling" of Gly172 results *intrinsically* from electrostatic changes that occur along the reaction pathway of BcX as Glu78 alternates between its negatively charged nucleophilic and neutral covalently modified states.

A major challenge is to delineate the factors establishing the precise pK_a values of ionizable groups in proteins, as required to understand catalytic mechanisms, to develop algorithms to accurately predict the complex electrostatic interactions within these molecules, and to engineer their pH_{opt}. To this end, we quantitatively dissected several factors that help set the pK_a values of the catalytic glutamic acid residues in BcX, including hydrogen bonding and Coulombic interactions with neighboring charged groups.[11] Furthermore, by systematically mutating core active site residues, we demonstrated that the pK_a values of Glu78 and Glu172, and hence the pH_{opt} of BcX, could be shifted by more than ±1 log units. Not surprisingly, the changes usually occurred at the cost of reduced catalytic activity. However, in one striking case, substitution of Asn35, adjacent to Glu172, with an Asp both reduced the pH_{opt} of BcX to 4.6 and increased its activity by ∼20%.[12] Indeed, the presence of an Asn or Asp residue at this position is a key determinant of the high or low pH_{opt} of GH-11 xylanases, respectively.[9] Detailed analyses revealed that this N35D mutant follows a "reverse protonation" mechanism,[13] being catalytically active when Asp35, with a *lower* pK_a of 3.5, is protonated to help serve as a general acid, while the nucleophile Glu78, with a *higher* pK_a of 5.8, is deprotonated. Only a small fraction of the mutant enzyme is ever in its catalytically competent ionization state, and thus this state must have an intrinsic efficiency significantly greater than that of WT-BcX. This efficiency can be explained by the increased hydrogen bonding strength of the Asp35-Glu172 dicarboxyl pair in the reaction transition state, as seen in the crystal structure of the resulting covalent glycosyl-enzyme intermediate.[12]

In this study, we have continued to explore strategies for manipulating the pK_a values of Glu78 and Glu172 and thereby altering the pH-dependent activity of BcX. We show that simply changing the global charge of BcX by random succinylation of surface lysine and tyrosine residues does not significantly change its pH_{opt}. Also, mutation of an extensive set of "second shell" residues that are near or within the active site of BcX, but not directly contacting the catalytic Glu78 and Glu172, either had little effect or modestly reduced the pH_{opt} of BcX. The latter resulted primarily from a lowering of the pK_a value of Glu78, and surprisingly occurred with the introduction of either positively or negatively charged groups. However, as with the previous study of "first shell" residues,[11] the mutations that caused the largest pK_a changes also significantly reduced the activity of BcX. This likely results from subtle structural or electrostatic perturbations and indicates that single site mutations of even second shell residues will most likely have detrimental effects on catalysis. Remarkably, substitution of the catalytic Glu172 with a histidine reduced the pH_{opt} of BcX by ∼1 unit. Although not used as a general acid/base residue in naturally occurring GH-11 xylanases, the E172H mutant retained 8% activity toward a xylobiose substrate. Furthermore, as with the previously described N35D variant, mutation of Asn35 to either histidine or glutamic acid also led to a reduced pH_{opt}. Detailed pK_a measurements by NMR spectroscopy revealed that, despite the opposite charges of the mutated residues, both the N35H and N35E forms of BcX also utilize a reverse protonation mechanism. Collectively, this study illustrates possible routes for altering the pH-dependent properties of GH-11 xylanases, while also highlighting the challenges associated with predicting or rationalizing the effects of mutations on its pH-dependent properties.

MATERIALS AND METHODS

Mutagenesis. The synthetic gene encoding WT-BcX was cloned into the pCW plasmid system under the control of an inducible *tac* promoter.[14] The genes encoding N35D- and N35E-BcX were generated by site-directed mutagenesis using the Kunkel method.[12,15,16] The synthetic WT-BcX gene was also cloned into pET22b (Novagen, EMD Biosciences) followed by QuikChange site-directed mutagenesis (Stratagene) to create the remaining mutants used in this study. All resulting plasmids were verified by DNA sequencing.

Protein Expression and Purification. Protein production and purification was performed as outlined previously.[11,14] pCW- and pET22b-encoded proteins were expressed primarily in *E. coli* Tuner (λDE3) pLysS and *E. coli* BL21 (λDE3) cells (Novagen), respectively. LB medium was used to produce unlabeled BcX, and M9 medium with 1 g/L $^{15}NH_4Cl$ and/or 3 g/L $^{13}C_6$-glucose (Spectra Stable Isotope Inc.) to produce uniformly ^{15}N- and/or ^{13}C-labeled protein. Selectively labeled BcX was produced using *E. coli* DL39 *avt*A::Tn5 cells[17] or *E. coli* BL21 *hisG*::Tn10 (λDE3)[18] grown in a synthetic medium[19] containing 300 mg/L of 99% L-δ-^{13}C-glutamate (Isotec) or 50 mg/L 98% L-$^{13}C_6$-$^{15}N_3$-histidine (Sigma-Aldrich), respectively. After growth at 30 or 37 °C to an OD_{600} ∼ 0.6, protein expression was induced overnight with IPTG (1 mM final for pCW plasmids and 0.05−0.1 mM for pET22b plasmids, the latter being reduced to avoid inclusion body formation). Proteins were purified with SP-Sepharose ion exchange chromatography (10 mM sodium phosphate buffer pH 6.0; 0−1 M NaCl gradient). In the case of samples for NMR analysis, Sephacryl S-100 size exclusion chromatography (10 mM sodium phosphate buffer pH 6.0, 150 mM NaCl) was also utilized for additional purification. Samples of covalently

dx.doi.org/10.1021/bi400034m | *Biochemistry* 2013, 52, 3138−3156

Table 1. X-ray Crystallographic Statistics

	E172H	E172H-2FXb	N35E	N35E-2FXb	E35H	N35H-2FXb
Data						
space group	$P2_1$	$P2_12_12_1$	$P2_1$	$P2_1$	$P2_1$	$P2_12_12_1$
monomers/asym unit	4	1	2	2	4	1
unit cell (Å, deg)	a = 52.1	a = 43.4	a = 39.3	a = 39.3	a = 52.4	a = 53.2
	b = 86.7	b = 52.3	b = 63.8	b = 63	b = 86.5	b = 72.2
	c = 73.0	c = 77.7	c = 64.1	c = 64.0	c = 69.8	c = 43.3
	β = 89.8		β = 104.5	β = 104.5	β = 90.02	
resolution range (Å)	38−2.4	30−1.8	62−1.54	60−1.67	30−2	60−1.7
highest shell (Å)	2.5−2.4	1.9−1.8	1.6−1.5	1.7−1.6	1.9−2	1.8−1.7
unique reflections	35327	15576	62680	49715	58218	23696
$I/\sigma(I)$	1.9	1.8	2.1	1.8	1.9	1.9
R_{sym} (%)	46	32	35	41	39	29
Refined model						
resolution range (Å)	38−2.4	20−1.8	30−1.5	30−1.6	17−2.0	30−1.7
no. reflections	15479	12533	40811	32247	37754	16514
R_{factor}/R_{free} (%)	23.8/34.4	17.2/25.4	16.1/19.6	18.8/23.5	21.0/26.6	16.4/19.9
mean B value (Å^2)	34	29	31	24	23	18
bond length rmsd (Å)	0.008	0.023	0.024	0.023	0.022	0.012
bond angles rmsd (deg)	1.3	1.8	1.9	1.9	1.9	1.8
accession code	3VZJ	3VZM	3VZK	3VZN	3VZL	3VZO

inhibited BcX were generated by incubation with a 2-fold molar excess of DNP2FX2.[20] SDS-PAGE and ESI-MS were used to verify protein identity, purity, and integrity. BcX concentrations were determined by absorbance spectroscopy using predicted ε_{280} values (http://ca.expasy.org/tools/protpar-ref.html).

Chemical Modification. Y88D-BcX was randomly succinylated by incubation of 3 mg/mL protein with 1 mg/mL succinic anhydride (Sigma) in 1 M Na_3BO_3 pH 8.0 at room temperature. The succinic anhydride was added with stirring during a period of 30 min, while keeping the pH ∼ 8.0 by addition of 0.1 M NaOH. The reaction mixture was stirred for an additional 15 min, then dialyzed against 10 mM Tris-HCl pH 8.0, and fractionated by anion exchange chromatography (10 mM Tris-HCl pH 8.0, 0−1 M NaCl gradient). The extent of modification of the protein present in each resolved peak was determined by ESI-MS.

Enzymatic Analysis. Steady-state Michaelis−Menten k_{cat} and K_m parameters were determined with ONPX2 as a substrate in 100 mM sodium phosphate pH 6.0, 0.1% BSA at 25 °C, according to methods described previously.[11] The pH dependence of k_{cat}/K_m was determined by the substrate-depletion method using ONPX2 (0.35 mM) in 50 mM NaCl, 0.1% BSA, and the appropriate buffer for each given pH range (3.0−4.5, 20 mM succinate; pH 5.0−6.5, 20 mM MES; pH 7.0−8.0, 20 mM HEPES; pH 8.5−10.0, 20 mM CHES). The apparent pK_a values corresponding to the acidic (pK_{a1}) and basic limbs (pK_{a2}) were determined by nonlinear least-squares fitting of the resulting bell-shaped k_{cat}/K_m versus pH profile to eq 1:

$$\left(\frac{k_{cat}}{K_M}\right)_{obs} = \left(\frac{k_{cat}}{K_M}\right)_{max} \left(\frac{1}{1 + (10^{-pH}/10^{-pK_{a1}}) + (10^{-pK_{a2}}/10^{-pH})}\right) \quad (1)$$

The reported standard errors (fit precision) were obtained via a Monte Carlo approach using the χ^2 of the initial fit to estimate the k_{cat}/K_m error and an assumed error of ±0.05 units for the sample pH values.

NMR-Monitored pH Titrations. NMR spectra were recorded at 25 °C with Varian 500 MHz Unity and cryoprobe-equipped 600 MHz Varian Inova and Bruker Avance III spectrometers, and processed with Topspin 3.1, NMRpipe[21] and Sparky.[22] Chemical shifts were referenced indirectly using external DSS (4,4-dimethyl-4-silapentane-1-sulfonic acid). Starting samples were typically ∼0.7 mM protein in 10 mM sodium phosphate pH 6.0. Sample pH values were adjusted by addition of small aliquots of 0.1−1.0 M NaOH or HCl, as appropriate, and measured at room temperature (∼ 20 °C). Histidine titrations were monitored in uniformly $^{13}C/^{15}N$-labeled protein samples using multiple-bond ^{15}N-HMBC[23] and one-bond sensitivity-enhanced ^{13}C−CPMG-HSQC experiments[24,25] optimized for the well-resolved $^{13}C^{\varepsilon1}$-$^{1}H^{\varepsilon1}$ correlations. Additional titrations of selectively $^{13}C_6/^{15}N_3$-histidine-labeled E172H-BcX were monitored with ^{13}C-HSQC, one-bond and multiple-bond ^{15}N-HSQC, and $H^{\beta}(C^{\beta})C^{\gamma}$ [26] experiments. Glutamic acid titrations were measured either by direct 1D ^{13}C NMR spectroscopy of selectively δ-^{13}C-Glu labeled N35H-BcX and E172H-BcX,[10] or by 2D ^{1}H-detected $^{1}H^{\gamma}(^{13}C^{\gamma})^{13}C^{\delta}$ and ^{15}N-HSQC correlation experiments recorded with uniformly $^{13}C/^{15}N$-labeled N35E-BcX.[27,28] Assignments were based on those reported previously for WT-BcX,[10,29,30] and augmented with 3D $C^{\gamma}C^{\beta}$-C^{δ}-$(C^{\gamma})H^{\gamma}$, C(CO)-TOCSY-NH, H(CCO)TOCSY-NH, and HNCACB spectra.[31]

pK_a values were obtained from nonlinear least-squares fitting of the measured pH-dependent chemical shifts to the equations describing 1, 2, or 3 macroscopic protonation equilibria, as discussed in detail elsewhere.[32] Fitting errors were estimated by a Monte Carlo approach using the χ^2 of the initial fit to estimate the chemical shift error and an assumed error of ±0.05 units for the sample pH values. Calculations were carried out using MathWorks Matlab, Kaliedagraph, and GraphPad Prism.

X-ray Crystallography. Crystals of N35E-, N35H-, and E172H-BcX, were grown at 18 °C using the hanging drop method by equilibrating 2 μL of purified protein solution (15−25 mg/mL) against an equal volume of 13−20% saturated

dx.doi.org/10.1021/bi400034m | Biochemistry 2013, 52, 3138−3156

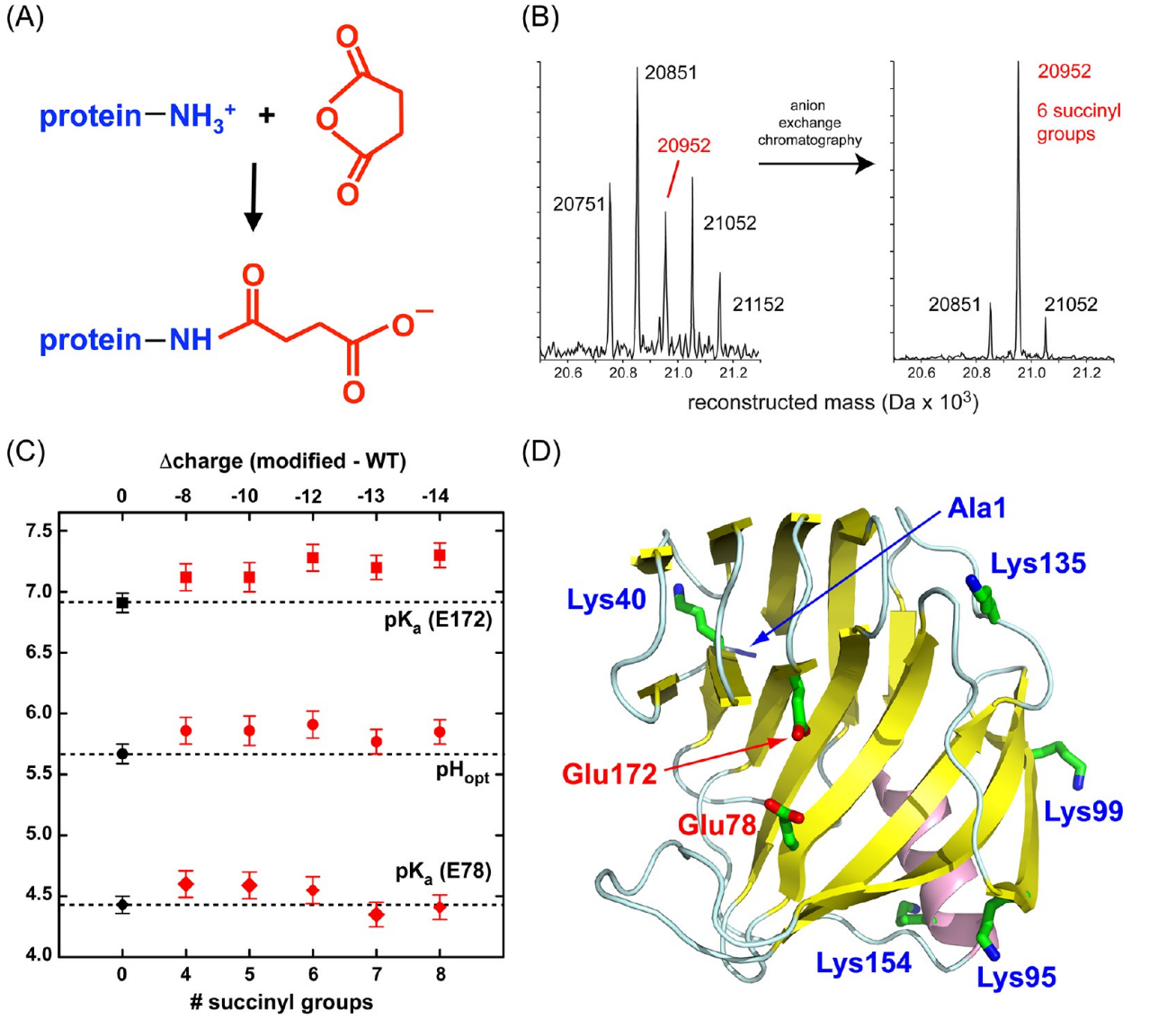

Figure 1. (A) Changing the global charge of BcX by succinylation does not significantly perturb its pH-dependent activity. (B) Reconstructed ESI-MS spectra of randomly succinylated Y88D-Bcx and of one fraction resolved by anion exchange chromatography (Δmass = 100 Da per succinyl group added). (C) Fit pH_{opt} and pK_a values assigned to Glu78 and Glu172 from the pH-dependence of k_{cat}/K_m for each species (Table 2). Dashed lines indicate the values for the unmodified protein. The net charge change assumes preferential modification of amines followed by tyrosine hydroxyls, and charges of +1 (amines), 0 (tyrosines), and −1 (succinyl carboxylates) at neutral pH. (D) Structure of BcX showing the positions of five Lys residues and the N-terminus relative to the catalytic Glu78 and Glu172 (carbon, green; oxygen, red; nitrogen, blue).

$(NH_4)_2SO_4$ in 40 mM Tris-HCl, pH 7.0 to 8.0. In the cases of the N35H- and E172H mutants, the drops were seeded with crystals obtained initially at 4 °C. To form the corresponding 2-deoxy-2-fluoro-β-xylobiosyl (2FXb) intermediates, DNP2FXb (~5 mM) was soaked into the crystals for time periods ranging from minutes to overnight. Better results were obtained after 3−5 h at room temperature, as longer times produced apparent surface stress and cracking. Crystals were serially transferred for a few seconds in mother liquor supplemented with increasing concentrations of glycerol (from 5 to 25%) and then frozen in liquid nitrogen. X-ray data collection was performed under cryogenic conditions (100 K) using an in-house RIGAKU 007HF rotating anode X-ray generator (Cu Kα radiation λ = 1.541 Å). Data were recorded using a MAR345 image plate detector, and processed using HKL2000.[33]

Molecular replacement was performed using PHASER[34] with the coordinates 1HV1.pdb as a search model. Subsequent model rebuilding and structure refinement were performed with CNS[35] (simulated annealing) and REFMAC[36] (maximum likelihood functions), alternating with manual adjustments using COOT.[37] The free R factor was calculated using a random ~5% of the total number of reflections that were excluded from the refinement. Tight noncrystallographic symmetry restraints and geometry were maintained throughout all the different steps of refinement and then partially relaxed at the final stage. Water molecules were assigned to 3σ residual ($F_o - F_c$) electron density areas within 3 Å of the protein. All models displayed acceptable stereochemical geometries, with >95% of residues in the most favorable regions of the Ramachadran plot. Table 1 provides a summary of these crystallographic analyses. The coordinate files have been deposited in the RCSB Protein Data Bank under the accession codes listed in Table 1.

dx.doi.org/10.1021/bi400034m | *Biochemistry* 2013, 52, 3138−3156

Table 2. pH-Dependent k_{cat}/K_M Values for the Hydrolysis of ONPX2 by Succinylated Y88D-BcX[a]

no. succinyl groups[b]	pK_{a1}[c]	pK_{a2}[c]	pH_{opt}[d]	(k_{cat}/K_M)[e] (s^{-1} mM^{-1})	rel activity[f]
0	4.43 ± 0.07	6.91 ± 0.08	5.67 ± 0.04	0.87 ± 0.03	1
4	4.58 ± 0.1	7.13 ± 0.1	5.86 ± 0.05	0.82 ± 0.03	0.94 ± 0.05
5	4.59 ± 0.1	7.12 ± 0.1	5.86 ± 0.06	0.65 ± 0.03	0.75 ± 0.04
6	4.55 ± 0.1	7.28 ± 0.1	5.91 ± 0.06	0.71 ± 0.03	0.82 ± 0.04
7	4.35 ± 0.1	7.20 ± 0.1	5.77 ± 0.05	0.94 ± 0.04	1.07 ± 0.06
8	4.41 ± 0.1	7.30 ± 0.1	5.85 ± 0.06	0.91 ± 0.04	1.04 ± 0.06

[a] k_{cat}/K_M data were determined from substrate depletion experiments carried out at 25 °C. Data for unmodified Y88D-BcX differ slightly from those in Table 3 due to different protein preparations and sample conditions. [b] Values are for the major species in the fractionated protein, based on ESI-MS analysis. [c] Apparent pK_a values were determined by fitting the data to the bell-shaped activity profiles of k_{cat}/K_M versus pH. The acidic limb (pK_{a1}) is attributed to the nucleophile Glu78 and the basic limb (pK_{a2}) is attributed to the acid/base catalyst Glu172. [d] $pH_{opt} = (pK_{a1} + pK_{a2})/2$. [e] Interpolated at the pH_{opt} for each species from the fit of k_{cat}/K_M versus sample pH value. This is slightly less than $(k_{cat}/K_M)_{max}$ in eq 1 due to a distribution of ionization states. [f] Ratios are based on the (k_{cat}/K_M) values at the pH_{opt} of each variant relative to unmodified Y88D-BcX at its pH_{opt}.

RESULTS

Activity Is Independent of Global Charge. To investigate the effect of global electrostatics on activity, we randomly succinylated Y88D-BcX, generating products varying in net charge at neutral pH by −2 for each amine (lysine or N-terminus) or −1 for each tyrosine modified (BcX has no cysteines). This mutant, with slightly higher activity than WT-BcX, was chosen due to its availability in large quantities. The reaction mixture was fractionated by ion exchange chromatography into populations having 4−8 succinyl groups, as measured by ESI-MS (Figure 1). The amino-terminal N of Ala1 and the side chain N^{ζ} of all 5 Lys residues in BcX are solvent exposed, although that of Lys40 may be partially protected by intramolecular hydrogen bonds. Similarly, the O^{η} of at least 11 out of 15 Tyr residues are accessible.[38] Under the experimental conditions, succinic anhydride reacts more readily with amines than phenols.[39] Thus, we assume that populations of BcX with 4, 5, or 6 succinyl groups were amine-modified, with charge changes of up to −8, −10, and −12, respectively, whereas the seventh and eighth succinyl groups were on tyrosines, for total charge changes of −13 and −14, respectively. This corresponds to a decrease in predicted isoelectric point (pI) from ∼9 for native BcX to ∼4.5 for the most modified species.

Despite the extensive net charge changes, each population of randomly succinylated Y88D exhibited similar pH-dependent activity profiles and k_{cat}/K_m values to that of the unmodified parent (Figure 1 and Table 2). The pH_{opt} of the enzyme increased only slightly upon modification ($\Delta pH_{opt} < 0.25$) due to small changes in the apparent pK_a values describing the acidic limb ($\Delta pK_a < 0.2$) and basic limb ($\Delta pK_a < 0.4$) of its bell-shaped activity profiles. These apparent pK_a values are attributed to Glu78 and Glu172, respectively. Recognizing that the pK_a value of the succinyl carboxyl is ∼4.5,[40] the marginally greater effect of these modifications on Glu172 might reflect a larger net negative (and hence repulsive) electrostatic charge change within the active site under pH conditions near its pK_a value of ∼7 than near the pK_a value of ∼4.5 for Glu78. Although the modest effects of random succinylation are not unexpected, given that the amines are solvent exposed and 15−25 Å away from either catalytic Glu, these results clearly show that the pH-dependent activity of BcX is not established simply by its global electrostatic properties. Parenthetically, given that the k_{cat}/K_m value for BcX does not markedly change with random succinylation at even eight positions, it is unlikely that any of the active site tyrosines are modified to a significant level.

"Second Shell" Mutations Perturb pH-Dependent Activity. With the exception of the previously described N35D variant,[41] mutation of residues in BcX directly contacting Glu78 or Glu172 led to shifted pH_{opt} at the price of reduced activities.[11] In contrast, changing its global charge has no marked effect. Thus, we tested whether the pH_{opt} of BcX could be manipulated by adding/removing ionizable groups "one layer" from its core active site to electrostatically, but not structurally, perturb the catalytic Glu78/172. To test this hypothesis, we introduced Asp, Glu, His, or Lys residues at positions flanking the active site of BcX. These loosely defined "second shell" positions were selected using the simple criteria of being within ∼6−15 Å of both Glu78 and Glu172, and in most cases, solvent exposed (Figure 2). For completeness, the "first shell" Gln127, which hydrogen bonds to Glu78, was also mutated to a histidine.

The pH-dependent catalytic properties of the generated mutants are summarized in Table 3 and Figure 2. Overall, the mutations changed the kinetically determined apparent pK_a value attributed to Glu87 by +0.1 to ∼ −1.6 log units and that of Glu172 by +0.7 to −0.3, and thereby altered the pH_{opt} of Bcx by +0.1 to −0.9. However, within this data set, there is no obvious correlation with distance between the mutation sites and either catalytic residue. Furthermore, the introduction of both potentially negatively (Asp, Glu) and positively (Lys, His) charged residues led to reduced pH_{opt} values. The effect appears to arise primarily through a decrease in the pK_a value attributed to Glu78. This stands in contrast to the results of succinylation, suggesting that the changes arise not through simple electrostatic interactions (which depend upon the pK_a value of the introduced residue relative to those of Glu78 and Glu127) but also through possible perturbations in active site structure or solvation.

Although many of the mutations did not markedly change the activity of BcX toward ONPX2, several reduced the k_{cat}/K_m value for this substrate to <15% of that of the WT enzyme. Not surprisingly, the latter mutations also tended to have the greatest effects on the apparent pK_a values of Glu78 and Glu172. These include A115E and S117D in the thumb region alongside the active site, Q7K at one end of the active site, T67D at the "back" of the active site, and R112E and Q127H, which are adjacent to Glu78. Interestingly, Y88D increases activity by ∼3 fold, yet lies at the outer edge of the substrate binding cleft. Although not characterized structurally, presumably these mutations at least subtly perturb the catalytic residues of BcX. Regardless, these results confirm previous

dx.doi.org/10.1021/bi400034m | Biochemistry 2013, 52, 3138−3156

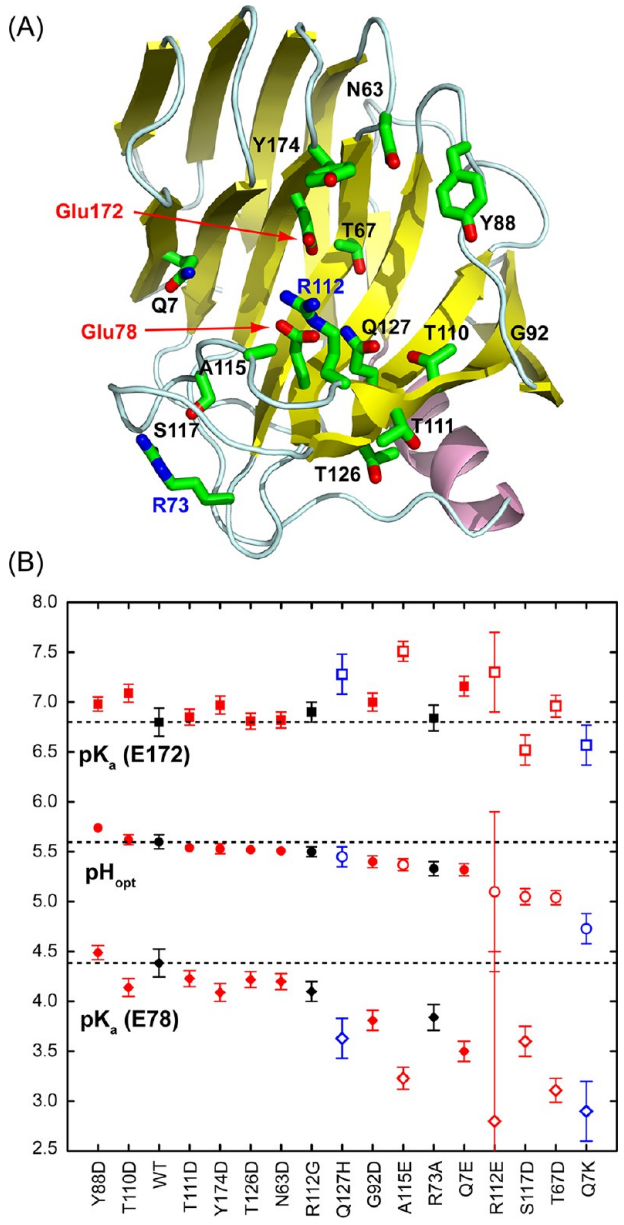

Figure 2. The effects of mutating "second shell" residues on the pH-dependent activity of BcX. (A) Mutated residues shown on the BcX structure. (B) Fit pH_{opt} and pK_a values assigned to Glu78 and Glu172 from the pH-dependence of k_{cat}/K_m for each species (Table 3). Mutations to Asp or Glu are colored in red, to His or Lys in blue, and to Ala or Gly in black. Open symbols identify mutants with relative activities <15%. Dashed lines indicate the values for WT-BcX. Some error bars, reflecting the fit precision, are smaller than the symbols.

observations that mutations, which significantly shift the pH_{opt} of this xylanase, generally also reduce its activity.

His172 Functions as a General Acid/Base Residue and Lowers the pH_{opt} of E172H-BcX. We also sought to change the pH-dependent activity of BcX through further mutation of its active site residues. Remarkably, despite its absolute conversation in naturally occurring GH-11 family members, mutation of Glu172 to a histidine resulted in an enzyme with 8% activity toward ONPX2 (Table 4 and Figure 3). The decreased activity is primarily due to reduction in k_{cat}, rather than K_m, value. Perhaps even more striking, the E172H variant has a pH_{opt} of 4.67, which is ~1 log unit less than that of WT-BcX. Fitting the pH-dependent k_{cat}/K_m profile yielded apparent pK_a values of 3.78 and 5.56 for the acidic and basic limbs of the bell-shaped curve, respectively. The simplest interpretation of these data is that the two pK_a values correspond to the Glu78 and His172, and that these residues serve as the catalytic nucleophile and general acid. It is also noteworthy that E172H-BcX exhibited some residual activity toward ONPX2 under alkaline conditions, suggesting a change in mechanism such as another residue assuming the role of acid catalyst, or a base-catalyzed process coming into play in this mutant.

To confirm the assignment of these kinetically determined pK_a values, derived from the pH-dependence of the second-order rate constant (k_{cat}/K_m) for the reaction of *free* enzyme and substrate, we exploited NMR spectroscopy to site-specifically probe the Glu and His residues in E172H-BcX (Figure 4 and Supplemental Table S1). Using ^{13}C-NMR to monitor the pH-dependent spectra of the $^{13}C^{\delta}$-glutamic acid labeled protein (Supplemental Figure S1), a biphasic titration curve was observed for Glu78. The major transition, attributed to the deprotonation of Glu78, fit to a pK_a value of 3.39, whereas the minor, attributed to perturbations from the titration of nearby His172, fit to an apparent pK_a value of 4.96. Conversely, the $^1H^{\varepsilon 1}$ of His172 followed a major titration with a pK_a value of 5.22, assigned to its own deprotonation, and a minor value of 3.46 that likely reflects the behavior of Glu78. The approximate agreement of these NMR-measured pK_a values for Glu78 and His172 and their correspondence with the apparent pK_a values governing the activity profile of E172H-BcX provide strong support for the proposed catalytic role of His172 as a general acid (Table 4).

It is very unusual that the NMR signals from the $^{13}C^{\varepsilon 1}$ and $^1H^{\varepsilon 1}$ of His172 in E172H-BcX did not shift colinearly with sample pH (Figure 4). As a result, fitting the $^{13}C^{\varepsilon 1}$ titration curve yielded an apparent pK_a value of ~3.4 for His172, which differs substantially from the above-noted major value of 5.22 reported by its $^1H^{\varepsilon 1}$. In contrast, the $^{13}C^{\varepsilon 1}$ and $^1H^{\varepsilon 1}$ of His156 shifted exactly colinearly with pH, and both yielded an unperturbed pK_a value of ~6.0 for this surface exposed residue. To resolve this surprising discrepancy, we also monitored the pH-dependent chemical shifts of essentially all applicable ^{1}H, ^{13}C, and ^{15}N reporter nuclei in a sample of E172H-BcX selectively labeled with $^{13}C_6/^{15}N_3$-histidine. As documented in Supplemental Figures S2 and S3, the $^{13}C^{\alpha}$, $^{13}C^{\beta}$, and $^{13}C^{\delta 2}$ of His172 also showed biphasic behavior with major titrations pK_a values of ~5.3. Furthermore, at pH 3.93, its ring $^{15}N^{\delta 1}$ and $^{15}N^{\varepsilon 2}$ have chemical shifts highly characteristic of protonated histidine side chain, thus excluding a possible pK_a value as low as ~3.4. Collectively, these data confirmed that the pK_a value of His172 in E172H-BcX is ~5.2 to 5.3, and that the additional spectral changes, including those dominating its $^{13}C^{\varepsilon 1}$ titration curve, most likely arise from perturbations due to the titration of nearby Glu78.

As discussed in detail elsewhere, biphasic titration curves for two electrostatically coupled ionizable residues can also be fit to yield four microscopic pK_a values governing their ionization equilibria.[32] Such fitting does require the assumption that the chemical shift of each residue is dependent only upon its own ionization, and that the deviations from a simple Henderson–Hasselbalch titration curve reflect the relative populations of species along their branched ionization pathways. In contrast, the fitting presented in Figure 4 yields macroscopic pK_a values reflecting the average behavior of the system. With this caveat

dx.doi.org/10.1021/bi400034m | *Biochemistry* 2013, 52, 3138–3156

Table 3. pH-Dependent k_{cat}/K_M Values for the Hydrolysis of ONPX2 by "Second Shell" Mutants of BcX[a]

mutant	pK_{a1}[b]	pK_{a2}[b]	pH_{opt}[c]	(k_{cat}/K_M)[d] (s^{-1} mM^{-1})	rel activity[e]
WT	4.39 ± 0.14	6.80 ± 0.14	5.60 ± 0.07	0.33 ± 0.02	1
Q7E	3.50 ± 0.10	7.16 ± 0.10	5.32 ± 0.06	0.093 ± 0.004	0.28 ± 0.02
Q7K	2.90 ± 0.30	6.57 ± 0.2	4.73 ± 0.15	0.0013 ± 0.0001	0.004 ± 0.0004
N63D	4.20 ± 0.08	6.82 ± 0.08	5.51 ± 0.04	0.36 ± 0.01	1.10 ± 0.08
T67D	3.11 ± 0.12	6.96 ± 0.11	5.04 ± 0.07	0.038 ± 0.002	0.12 ± 0.008
Y88D	4.49 ± 0.07	6.98 ± 0.07	5.74 ± 0.04	1.01 ± 0.03	3.06 ± 0.20
R73A	3.84 ± 0.13	6.84 ± 0.13	5.33 ± 0.07	0.14 ± 0.01	0.41 ± 0.03
G92D	3.81 ± 0.10	7.00 ± 0.09	5.40 ± 0.06	0.12 ± 0.005	0.37 ± 0.03
T110D	4.14 ± 0.09	7.09 ± 0.09	5.62 ± 0.05	0.41 ± 0.01	1.23 ± 0.09
T111D	4.23 ± 0.08	6.85 ± 0.08	5.54 ± 0.04	0.26 ± 0.01	0.79 ± 0.05
R112E	2.80 ± 1.7	7.30 ± 0.40	5.10 ± 0.80	0.0013 ± 0.0001	0.004 ± 0.0005
R112G	4.10 ± 0.10	6.90 ± 0.10	5.50 ± 0.05	0.56 ± 0.02	1.70 ± 0.12
A115E	3.23 ± 0.11	7.51 ± 0.10	5.37 ± 0.06	0.04 ± 0.001	0.12 ± 0.008
S117D	3.60 ± 0.15	6.52 ± 0.15	5.05 ± 0.08	0.008 ± 0.0005	0.024 ± 0.002
T126D	4.22 ± 0.08	6.81 ± 0.08	5.52 ± 0.04	0.29 ± 0.01	0.88 ± 0.06
Q127H	3.63 ± 0.2	7.28 ± 0.2	5.45 ± 0.10	0.003 ± 0.0002	0.01 ± 0.001
Y174D	4.09 ± 0.09	6.97 ± 0.09	5.53 ± 0.05	0.11 ± 0.004	0.34 ± 0.02

[a] k_{cat}/K_M data were determined from substrate depletion experiments carried out at 25 °C. [b] Apparent pK_a values were determined by fitting pH-dependent k_{cat}/K_m values to a bell-shaped activity profile. The acidic limb (pK_{a1}) is attributed to the nucleophile Glu78 and the basic limb (pK_{a2}) is attributed to the acid/base catalyst Glu172. [c] $pH_{opt} = (pK_{a1} + pK_2)/2$. [d] Interpolated at the pH_{opt} of each mutant from the fit of k_{cat}/K_M versus sample pH value. This is slightly less than $(k_{cat}/K_M)_{max}$ in eq 1 due to a distribution of ionization states. [e] Values are based on (k_{cat}/K_M) values at the pH_{opt} of each variant relative to WT-BcX at its pH_{opt}.

Table 4. Kinetic Parameters for the Hydrolysis of ONPX2 by WT and Active Site Mutant BcX Proteins

protein	k_{cat}[a] (s^{-1})	K_M[a] (mM^{-1})	(k_{cat}/K_M)[b] ($s^{-1}mM^{-1}$)	rel activity[c]	pH_{opt}[d]	pK_{a1}[e]	pK_{a2}[e]	pK_a[f] (E 78)	pK_a[f] (E/H 172)	pK_a[f] (H/E/D 35)
WT	1.3	3.4	0.33 ± 0.02	1	5.60 ± 0.07	**4.39 ± 0.14**	*6.80 ± 0.14*	**4.57 ± 0.07**	*6.74 ± 0.05*	
E172H	0.015	1.8	0.025 ± 0.002	0.08 ± 0.008	4.67 ± 0.04	**3.78 ± 0.1**	*5.56 ± 0.1*	**3.39 ± 0.09**	*5.22 ± 0.05*	
N35H	0.38	3.0	0.40 ± 0.008	1.21 ± 0.08	4.39 ± 0.03	**3.12 ± 0.06**	*5.65 ± 0.06*	*5.47 ± 0.04*	**3.39 ± 0.04**	7.48 ± 0.04
N35E	0.082	3.4	0.054 ± 0.002	0.16 ± 0.01	4.43 ± 0.05	**2.93 ± 0.1**	*5.92 ± 0.08*	*5.26 ± 0.05*	8.08 ± 0.02	**3.37 ± 0.09**
N35D[g]	1.8	12.5	0.43	1.2	4.6	**3.5**	*5.8*	*5.7*	8.4	**3.7**

[a] k_{cat} and K_M values were determined from a complete Michaelis–Menten kinetic analysis at pH 6.0 and 25 °C (Figure 3). Results differ slightly from those published previously due to differences in experimental conditions.[10,11] [b] k_{cat}/K_M data were determined from substrate depletion experiments at 25 °C, and the reported values interpolated to the pH_{opt} of each variant from the fit of k_{cat}/K_M versus sample pH. This is slightly less than $(k_{cat}/K_M)_{max}$ in eq 1 due to a distribution of ionization states. [c] Based on (k_{cat}/K_M) values at the pH_{opt} of each variant relative to WT-BcX at its pH_{opt}. [d] $pH_{opt} = (pK_{a1} + pK_{a2})/2$. [e] Apparent pK_a values were determined by fitting pH-dependent k_{cat}/K_m values to a bell-shaped activity profile. In the case of E172H, an offset was included to account for residual activity at high sample pH. [f] Major pK_a values determined from NMR-monitored pH-titrations for Glu78, Glu/His172, and His/Glu/Asp35 (see Supplemental Table S1 for a complete summary). The pK_a values matching those of the acidic limb (pK_{a1}) and basic limb (pK_{a2}) are highlighted in bold and italics, respectively. [g] Data from Joshi et al.[12]

in mind, fitting the pH-dependent $^{13}C^{\delta}$ chemical shift of Glu78 and $^{1}H^{\epsilon 1}$ chemical shift of His172 simultaneously yielded the microscopic pK_a values summarized in Figure 4D. According to this scheme, with increasing sample pH, the predominant ionization pathway involves deprotonation of Glu78 followed by His172 (with microscopic pK_a values of 3.51 and 5.11, respectively). However, an alternative pathway also can occur measurably, with His172 deprotonating before Glu78 (microscopic pK_a values of 4.26 and 4.36, respectively). The 0.85 unit difference between the pK_a values for each residue in the presence of its charged versus neutral partner corresponds to a favorable interaction energy of $-2.303RT(\Delta pK_a) \sim -1.2$ kcal/mol between Glu78 and His172. The unfavorable interaction energy between Glu78 and Glu172 in WT-BcX is of a comparable magnitude.[32] These data indicate that the microscopic pK_a value of Glu78 is reduced to ~3.5, and that of His172 raised to ~5.1, due to favorable electrostatic interactions. However, in the presence of neutral His172, Glu78 has a pK_a value of ~4.4, which is near its value in WT-BxC with a neutral Glu172 partner. Finally, the low microscopic pK_a value of ~4.3 for His172 (relative to ~6.5 for a random coil histidine[42]) when Glu78 is protonated indicates that its environment in the BcX active site favors the neutral imidazole side chain.

The X-ray crystallographic structure of E172H-BcX in its apo form supports these conclusions (Figure 5). Overall, the structure superimposes closely with that of WT-BcX, including the position of the partially buried nucleophile Glu78 (fractional side chain accessible surface area ASA ~ 0.1, and hydrogen bonded to Tyr69 and Gln127[43]). However, in contrast to the favorable hydrogen bonding interactions of Glu172 with Asn35 and Tyr80 observed in WT-BcX, the side chain of His172 shows variable conformations in the four monomers of the asymmetric unit. In each conformation, His172 is unable to hydrogen bond with any neighboring residues. On the basis of the pH-dependence of its $^{13}C^{\gamma}$ and $^{13}C^{\delta 2}$ chemical shifts, His172 is most likely in the neutral $N^{\epsilon 2}H$ tautomeric form under the crystallization conditions of pH 7 to 8. However, at pH > 6, the $^{13}C^{\delta 2}$-$^{1}H^{\delta 2}$ and $^{13}C^{\gamma}$-$^{1}H^{\beta\beta'}$ NMR signals of the histidine side chain were not detected (Supplemental Figure S2). This is suggestive of signal

dx.doi.org/10.1021/bi400034m | Biochemistry 2013, 52, 3138–3156

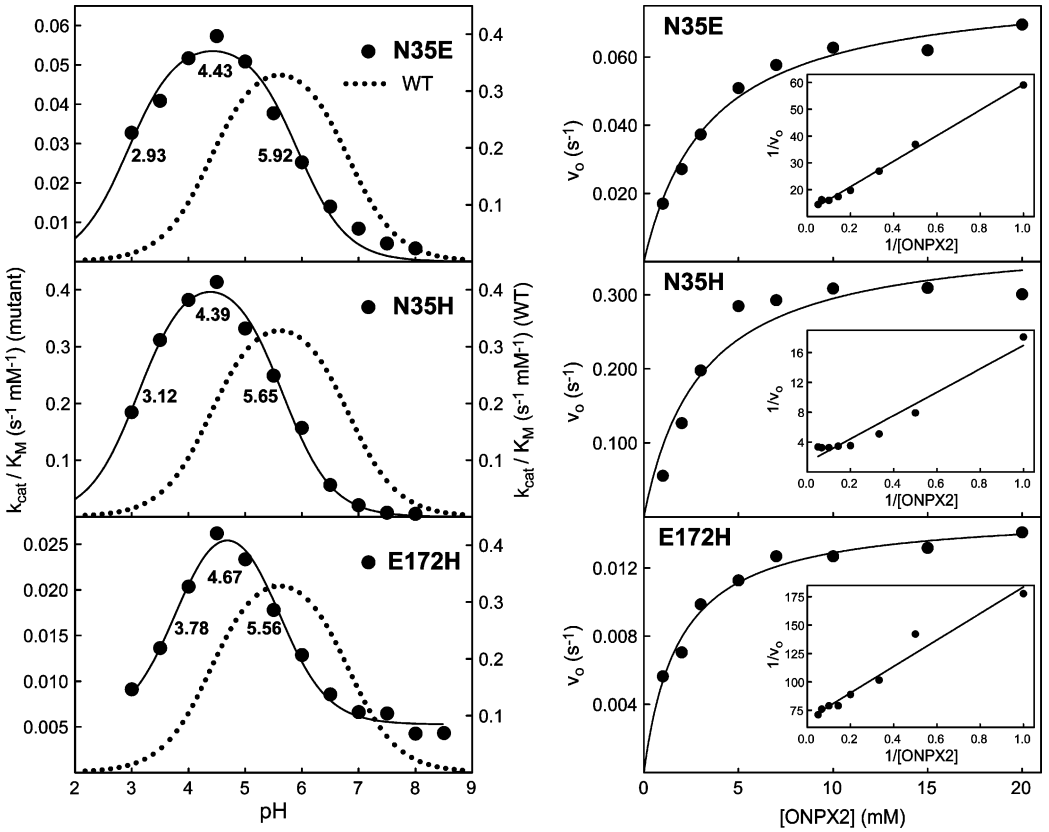

Figure 3. Kinetic characterization of the E172H, N35H, and N35E variants of BcX. Left: pH-dependence of k_{cat}/K_m (left *y*-axis) for the three mutants (•) as determined by ONXP2 substrate depletion. The numbers indicate the fit pK_a and pH_{opt} values (Table 4). The fit activity curve of WT-BcX is also shown for comparison (dotted line, right *y*-axis; pK_{aGlu78} = 4.39, p$K_{aGlu172}$ = 6.80, pH_{opt} = 5.60). Right: Michaelis–Menten curves for the three mutants at pH 6.0 and 25 °C. The systematic deviations of the corresponding Lineweaver–Burk plots (inset) from linearity likely arise from transglycosylation at high substrate concentrations.

broadening due to ms to μs time scale conformational exchange and/or tautomerization of neutral His172. Also consistent with the NMR-monitored titration data for E172H-BcX, the close proximity of Glu78 and His172 (~6 Å) should result in favorable electrostatic interactions, thereby lowering the pK_a value of the catalytic nucleophile and raising that of the general acid. However, its partially buried environment (fractional side chain ASA ~ 0.1) and lack of hydrogen bonding partners will reduce pK_a value of His172. The balance of these opposing effects likely leads to the overall reduction in the pH_{opt} of E172H-BcX relative to the WT parent.

E172H-BcX Exhibits pK_a Cycling upon Glycosyl-Enzyme Intermediate Formation. Treatment of WT-BcX with the mechanism-based inhibitor (or "slow substrate") DNP2FXb results in formation of a long-lived glycosyl-enzyme intermediate with the nucleophilic Glu78 covalently modified.[44] A similar modification occurs with E172H-BcX as evidenced by a pronounced change in the NMR signals of His172 (Figure 4 and Supplemental Table S1) and by X-ray crystallographic analysis (Figure 5). In contrast to the unmodified protein, the $^1H^{\varepsilon 1}$ and $^{13}C^{\varepsilon 1}$ of His172 show only slightly nonlinear pH titrations with apparent pK_a values of 2.80 or 3.11, respectively. Thus, upon glycosylation and hence neutralization of Glu78, the pK_a value of His172 drops from 5.22 to ~3.0. This phenomenon of pK_a cycling enables His172 to serve as a general base and facilitate nucleophilic attack of a water molecule during the deglycosylation step of the BcX catalytic reaction.[10] The decrease in the pK_a value of His172 by >2 log units is certainly in large part due to loss of a favorable electrostatic interaction with Glu78. However, is likely that changes in the solvation and structure of the active site also contribute as the fit microscopic pK_a value of 4.26 for His172 in the presence of a neutral Glu78 in the apo enzyme (Figure 4D) is substantially higher than that of ~3 measured in the covalently modified enzyme.

E172H-BcX reacted with DNP2FXb was also investigated by X-ray crystallography (Figure 5). Overall, its structure superimposed closely on that of the trapped WT glycosyl-enzyme intermediate. Because of a single S_N2 displacement, Glu78 bonded covalently to the 2FXb ligand via an α-glycosidic linkage. Importantly, the directly bonded proximal xylose in the −1 subsite adopted a distorted $^{2,5}B$ (boat) conformation, whereas the distal xylose in the −2 subsite had a conventional $^4C_1$ (chair) conformation. As discussed in detail previously,[20,45] the coplanarity of the C5, O5, C1, and C2 atoms of the proximal xylose will favor formation of an oxocarbenium ion-like transition state. In contrast to 2FXb-WT-BcX with Glu172 hydrogen bonded to Asn35, Tyr80, and a potential nucleophilic water, in 2FXb-E172H-BcX, His172 is hydrogen bonded to an alternatively placed water and to the O5 of the proximal xylose. Since His172 should be neutral under the crystallization conditions, this would require it to adopt the $N^{\varepsilon 2}H$ tautomeric state. Unfortunately we were unable to confirm this prediction using NMR spectroscopy as the $^{13}C^{\delta 2}$-$^1H^{\delta 2}$ and $^{13}C^{\gamma}$-$^1H^{\beta\beta'}$ signals of His172 in a $^{13}C_6/^{15}N_3$-histidine labeled sample were not detected in ^{13}C-HSQC and HB(CB)CG spectra,

dx.doi.org/10.1021/bi400034m | *Biochemistry* 2013, 52, 3138–3156

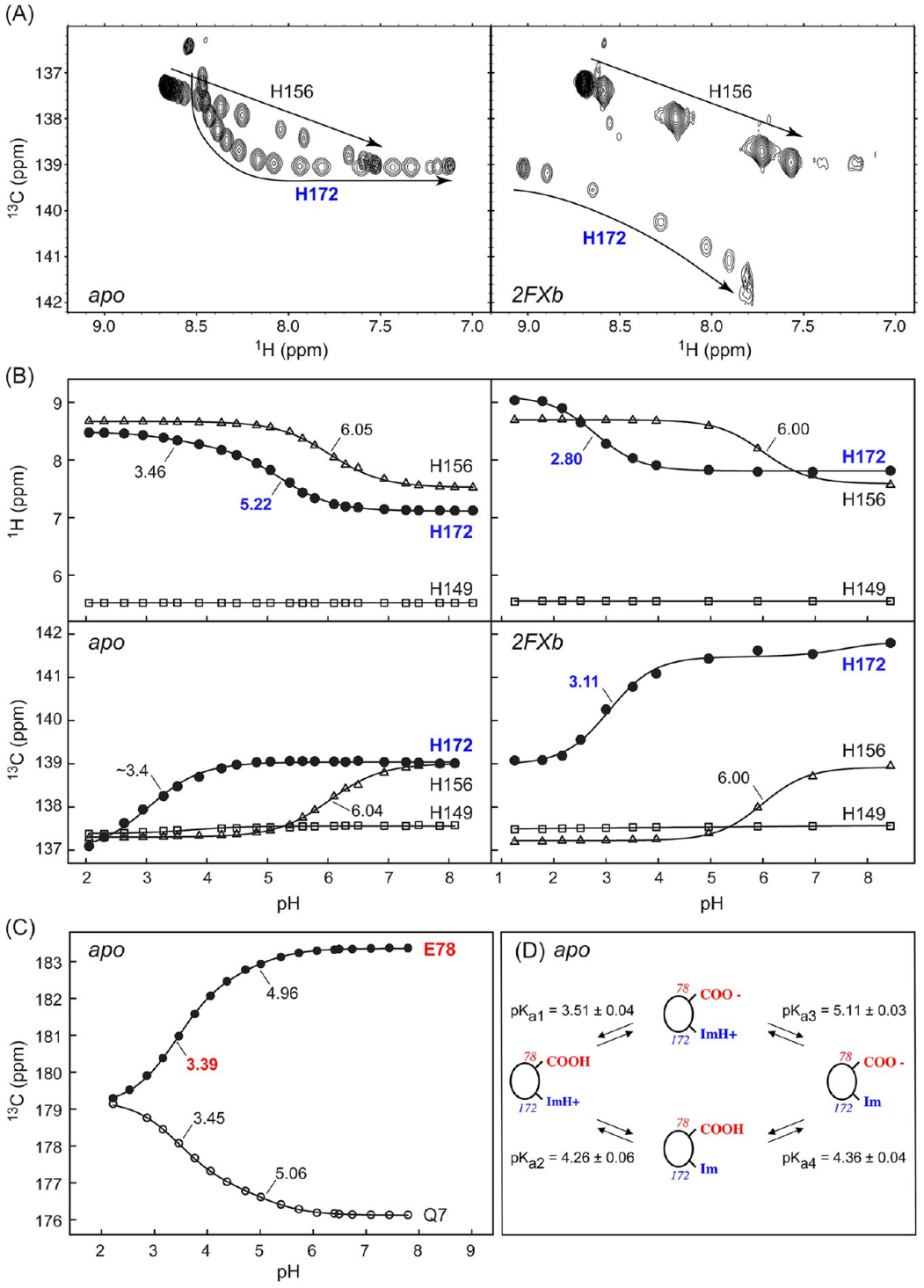

Figure 4. NMR monitored pH-titrations of E172H-BcX in its apo (left) and 2FXb-modified (right) forms. (A) Overlaid ^{13}C-HSQC spectra, showing the pH-dependent $^{13}C^{\varepsilon1}$-$^{1}H^{\varepsilon1}$ signals of His172 and His156 (arrows indicate increasing sample pH). The signal from His149 is not included. The weak peaks in the spectra of 2FXb-E172H are due to slow hydrolysis, yielding a minor amount of apo enzyme. (B) Fitting the pH-dependent $^{1}H^{\varepsilon1}$ (upper) and $^{13}C^{\varepsilon1}$ (lower) chemical shifts of His172 and His156 yields the indicated pK_a values. His149 is neutral over the entire pH range examined and thus confirms that the protein remains structured throughout the titration.[29] (C) Fitting the pH-dependent $^{13}C^{\delta}$ chemical shifts of Glu78 and the nonionizable reporter Gln7 (which primarily senses the ionization state of Glu78[10]) yields the indicated pK_a values for the apo enzyme. These data were obtained from the spectra shown in Supplemental Figure S1. In (B) and (C), the pK_a value assigned to the predominant titration of a given residue is highlighted in bold coloring. (D) Simultaneous fitting of the pH-dependent $^{13}C^{\delta}$ chemical shifts of Glu78 and $^{1}H^{\varepsilon1}$ chemical shifts of His172 to model of coupled ionizations yields the four indicated microscopic pK_a values. A detailed summary of the fit pK_a values, associated chemical shift changes, and errors is provided in Supplemental Table S1.

respectively, recorded between pH 2.5 and 5.9 (not shown). This suggests that His172 also undergoes ms to μs time scale conformational exchange broadening in the glycosyl-enzyme intermediate. Finally, a potential nucleophilic water for the

dx.doi.org/10.1021/bi400034m | *Biochemistry* 2013, 52, 3138−3156

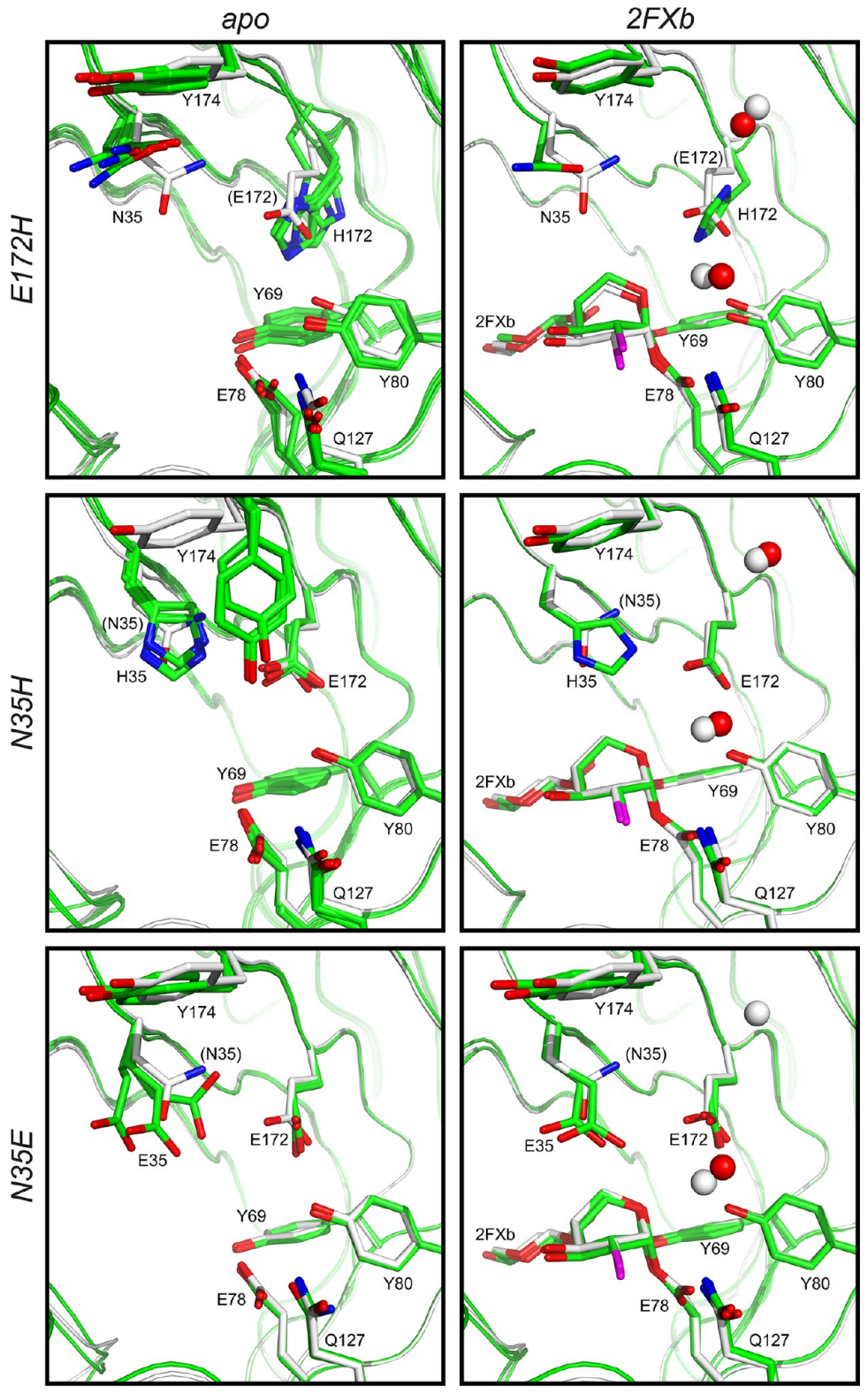

Figure 5. X-ray crystallographically determined structures of (top) E172H-BcX, (middle) N35H-BcX, and (lower) N35E-BcX in their (left) apo and (right) 2FXb glycosyl-enzyme intermediate forms, superimposed upon those of WT-BcX (pdb codes 1XNB and 1BVV, respectively). Selected residues are shown in stick format (carbon, green for mutant, gray for WT; oxygen, red; nitrogen, blue; fluorine, magenta), and bound waters as spheres (red for mutant, gray for WT). The four monomers from the asymmetric units of apo E172H-BcX and N35H-BcX, as well as the two from those of apo and 2FXb-modifed N35E-BcX are superimposed in this figure. Glu35 in one of the N35E-BcX monomers adopts two conformations. Note also that the rotomeric states of the Asn/Gln side chain amides and His imidazole ring were not determined unambiguously and thus could be flipped. Structural figures rendered with PyMol.[60]

dx.doi.org/10.1021/bi400034m | *Biochemistry* 2013, 52, 3138−3156

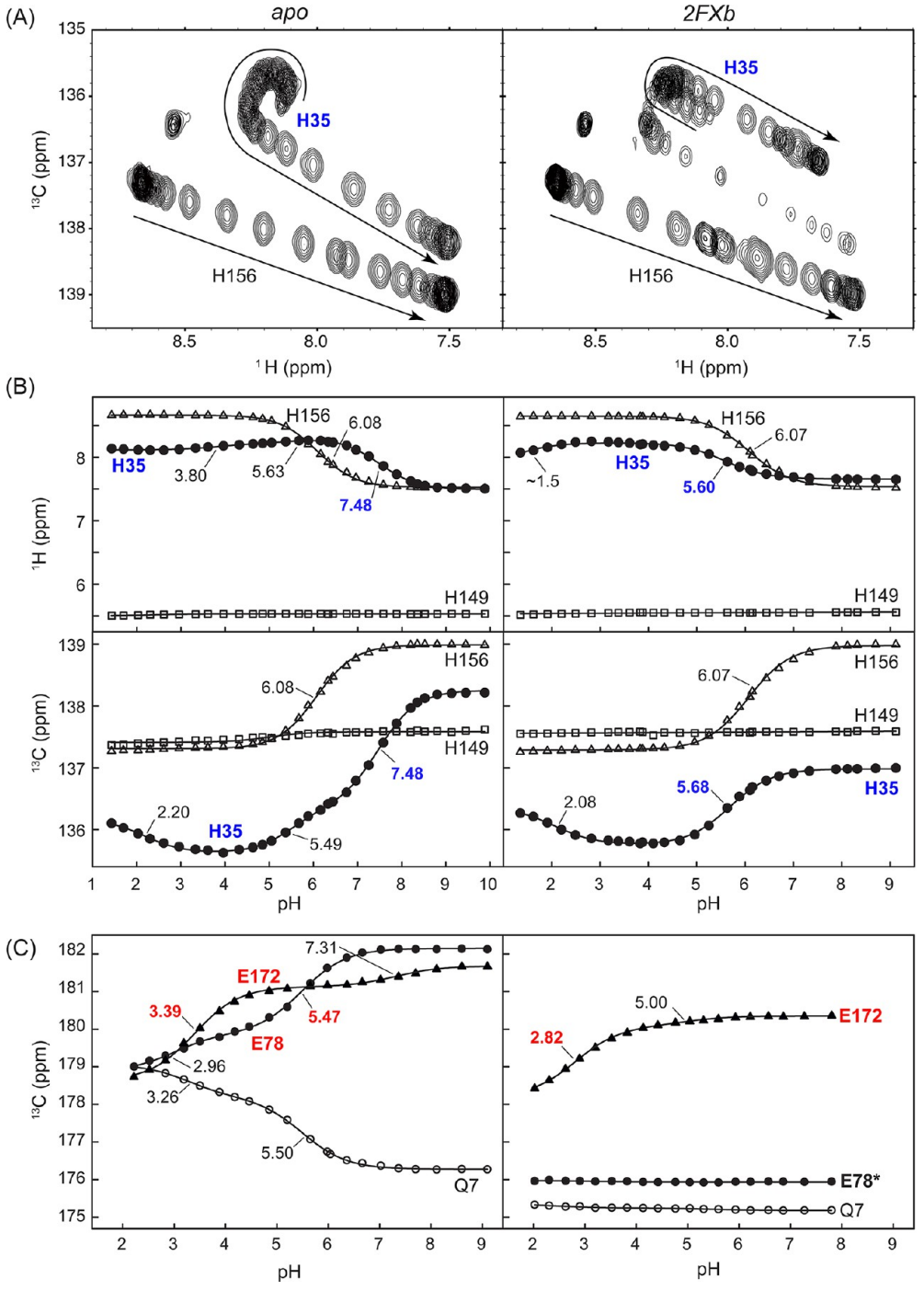

Figure 6. NMR monitored pH-titrations of N35H-BcX in its apo (left) and 2FXb-inhibited (right) forms. (A) Overlaid ^{13}C-HSQC spectra, showing the pH-dependent $^{13}C^{\epsilon 1}$-$^{1}H^{\epsilon 1}$ signals of His35 and His156 (arrows indicate increasing sample pH). The signal from His149 is not included. The weak peaks in the spectrum of 2FXb-N35H are due to slow hydrolysis, yielding a minor amount of apo enzyme. (B) Fitting the pH-dependent $^{1}H^{\epsilon 1}$ (upper) and $^{13}C^{\epsilon 1}$ (lower) chemical shifts of His35 and His156 yields the indicated pK_a values (see Table 4). His149 is neutral over the entire pH range examined and thus confirms that the protein remains structured throughout the titration.[29] (C) Fitting the pH-dependent $^{13}C^{\delta}$ chemical shifts of Glu78, Glu172 and the nonionizable reporter Gln7 (which primarily senses the ionization state of Glu78;[10]) yields the indicated pK_a values. E78* is the signal from the covalently modified Glu78. These data were obtained from the spectra shown in Supplemental Figure S4. In (B) and (C), the pK_a value assigned to the predominant titration of a given residue is highlighted in bold coloring. A detailed summary of the fit pK_a values, associated chemical shift changes, and errors is provided in Supplemental Table S1.

deglycosylation step was also observed in 2FXb-E172H-BcX crystal, albeit further from the proximal xylose C1 atom than in 2FXb-WT-BcX (4.8 Å versus 3.9 Å) and weakly hydrogen-bonded to only Tyr80.

It is noteworthy that the 2FXb ligand was best refined with only 50% occupancy, suggesting incomplete saturation of the inhibitor into the crystal (short soaking times were required to avoid cracking), slower formation of the glycosyl-enzyme intermediate, and/or more rapid hydrolysis relative to the case

dx.doi.org/10.1021/bi400034m | *Biochemistry* 2013, 52, 3138−3156

of WT-BcX. Either of the latter explanations are likely as E172H-BcX has impaired activity (although comparable to WT at pH 7 to 8, Figure 3), and, while not quantitatively measured, 2FXb-E172H-BcX hydrolyzed during NMR-monitored titrations notably faster than did the WT enzyme (Figure 4A). This faster turnover indicates that the deglycosylation step for the E172H mutant is relatively facile, despite the fact that the k_{cat} and k_{cat}/K_m values for this enzyme with ONPX2 are low. This implies that the glycosyl enzyme intermediate is less stable, relative to its flanking transition states, than is the case for the wild-type enzyme. This is not surprising since important active site interactions, such as those with Asn35, are disrupted by this mutation.

Substitution of Either His or Glu at Position 35 Reduces the pH_{opt} of BcX. Previously, we demonstrated that substitution of Asn35 (which directly contacts Glu172) with Asp significantly reduced the pH_{opt} of BcX to a value of 4.6, along with a small increase in activity.[12] This arises from a reverse protonation mechanism in which the Asp35-Glu172 dicarboxyl pair serves as the general acid with a pK_a value lower than that of the nucleophile Glu78. To further investigate this phenomenon, we introduced a Glu or His residue at position 35. As summarized in Table 4 and Figure 3, the resulting N35H-BcX variant exhibited ~20% increased activity toward ONPX2 and followed a bell-shaped k_{cat}/K_m versus pH curve with apparent pK_a values of 3.12 and 5.65 and a pH_{opt} of 4.39. Similarly, N35E-BcX displayed pK_a values of 2.93 and 5.92 and a pH_{opt} of 4.43, albeit with a moderately (16% versus WT) reduced activity due to a lower k_{cat} value. Thus, as with the initial N35D variant, either mutation shifted the activity profile of BcX by >1 log unit toward more acidic conditions. This result is somewhat surprising as His35 can be a positively charged residue near the catalytic Glu78 and Glu172, whereas Asp35 or Glu35 can be negatively charged, yet all three reduced the pH_{opt} of BcX. To understand these seemingly contradictory effects, we used NMR spectroscopy to monitor the pH-titrations of both mutants in their apo and trapped glycosyl enzyme intermediate states.

Reverse Protonation: His35 Reduces the pK_a of Glu172. The ionization equilibria of Glu78, Glu172, and His35 in N35H-BcX were investigated by measuring their pH-dependent $^{13}C^{\delta}$ and $^{13}C^{\varepsilon 1}$-$^{1}H^{\varepsilon 1}$ chemical shifts, respectively (Figure 6 and Supplemental Table S1). In all cases, multiphasic titration curves were observed, indicating interactions between the three residues. The $^{13}C^{\delta}$ of Glu78 exhibited a major titration with a pK_a value of 5.47, assigned to its own ionization. This conclusion is supported by a similar pK_a reported by Gln7, a residue at the edge of the BcX active site with a $^{13}C^{\delta}$ chemical shift that is particularly sensitive to the ionization state of Glu78.[10] Glu78 also showed a minor titration with a pK_a value of 2.96, attributable at least in part to perturbations by Glu172. Conversely, the $^{13}C^{\delta}$ of Glu172 followed a major titration with a pK_a value of 3.39 that is predominantly due to its own ionization, as well as a minor titration with a pK_a value of 7.31. The latter is attributed to His35. In a reciprocal fashion, the $^{1}H^{\varepsilon 1}$ and $^{13}C^{\varepsilon 1}$ of His35 showed its own titration at a pK_a value of 7.48, as well as smaller pH-dependent perturbations at pK_a values of 5.63 or 5.49, respectively, which likely arise from the ionization of Glu78. At lower sample pH values, the $^{13}C^{\varepsilon 1}$-$^{1}H^{\varepsilon 1}$ signals of His35 change in a highly nonlinear fashion, such that the $^{13}C^{\varepsilon 1}$ chemical shift follows a pK_a value of 2.20 whereas the $^{1}H^{\varepsilon 1}$ follows one at 3.80; the latter is likely due to Glu172. This perplexing behavior indicates that, as with E172H-BcX, the directly bonded $^{1}H^{\varepsilon 1}$ and $^{13}C^{\varepsilon 1}$ nuclei are sensitive to different pH-dependent changes in BcX.

Collectively, these measurements indicate that His35 has an elevated pK_a value of 7.48 and thus is positively charged under the more acidic conditions where N35H-BcX is active. As a result of this favorable electrostatic interaction, the pK_a value of adjacent Glu172 is reduced dramatically to 3.39. Concomitantly, the pK_a value of Glu78 is elevated to 5.47, suggesting that unfavorable interactions with Glu172 dominate over any favorable interactions with His35. The approximate correspondence of these latter two NMR-measured pK_a values with those determine kinetically indicates that the acidic limb of the bell-shaped activity profile of N35H-BcX is set by the general acid Glu172, whereas the basic limb is set by the nucleophile Glu78 (Table 4). This is opposite to the case of WT-BcX, and indicative of a reverse protonation mechanism in which the group with the lower pK_a value is the general acid and that with the higher value is the nucleophile. Therefore, at the pH_{opt} of N35H-BcX, only a small fraction is in the catalytically competent ionization state with the nucleophile deprotonated and the general acid still protonated.

Unfortunately, it was not possible to fit the titration curves of His35, Glu78, and Glu172 in terms of the eight microscopic pK_a values for three interacting ionizable residues as the system is underdetermined experimentally.[32] In particular, Glu78 and Glu172 did not show reciprocal perturbations, indicating that both their chemical shifts and ionization equilibria are dependent upon the charge state of one another. Thus, the simplifying assumption used in the case of E172H-BcX could not be applied.

Upon formation of a trapped glycosyl-enzyme intermediate, the covalently modified Glu78 no longer titrates, and Glu172 shows a dramatically reduced pK_a value of 2.82 (Figure 6 and Supplemental Table S1). Thus, as with WT-BcX, the pK_a value of Glu172 cycles along the reaction pathway to match its role as a general acid and then general base. The pK_a value of His35 also drops to 5.60 ($^{1}H^{\varepsilon 1}$ titration) or 5.68 ($^{13}C^{\varepsilon 1}$), likely due to the loss of a favorable electrostatic interaction with Glu78 or changes in active site hydration (or dielectric constant) resulting from the bound sugar. Again, at lower sample pH values, His35 shows a nonlinear $^{13}C^{\varepsilon 1}$-$^{1}H^{\varepsilon 1}$ chemical shift changes, with the two nuclei reporting distinct pK_a value of 2.08 and ~1.5, respectively. However, recognizing that it is difficult to reliably fit a pK_a value from a pH titration curve without well-defined end-points, these pK_a values likely reflect perturbations due to the ionization of Glu172 and/or to other Asp residues in the protein not monitored in this study.

The structures of N35H-BcX in its apo and 2FXb-trapped states were also determined by X-ray crystallography (Figure 5). Overall, the structures are closely superimposable upon those of the corresponding forms of the WT enzyme, including the $^{2,5}B$ skewed boat conformation of the 2FXb moiety covalently linked to Glu78 and a potential nucleophilic water.[20] In both cases, His35 directly hydrogen bonds to the Oε of Glu172 via its N$^{\varepsilon 2}$ (2.4−2.6 Å for apo, and 2.2 Å for 2FXb-modified). Also, Glu78 is ~6.5 Å from the side chain of His35 and ~7 Å from that of Glu172. The relative positions of these residues are consistent with the changes in their pK_a values versus those of the WT enzyme, as discussed above. Under the crystallization conditions of pH 7 to 8, His35 should be partially charged in the apo enzyme structure and neutral in the trapped glycosyl-enzyme intermediate, whereas the catalytic glutamates will be negatively charged in both forms. This

dx.doi.org/10.1021/bi400034m | Biochemistry 2013, 52, 3138−3156

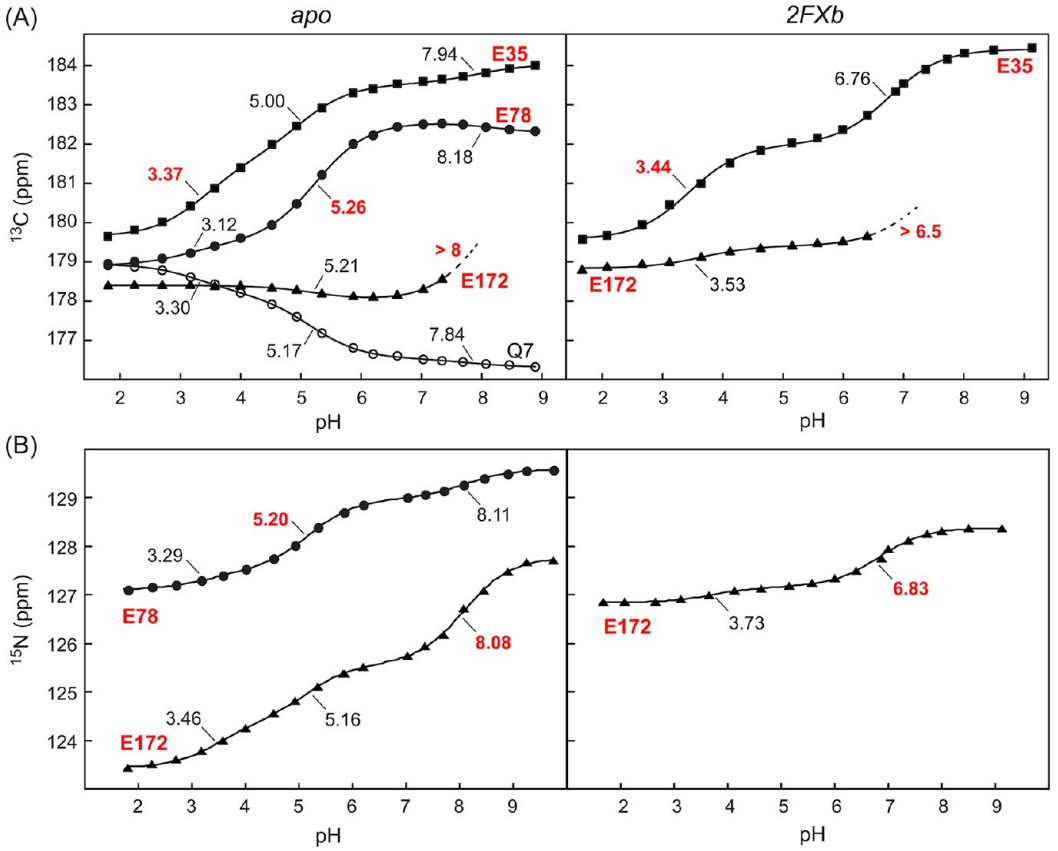

Figure 7. NMR monitored pH-titrations of N35E-BcX in its apo (left) and 2FXb-inhibited (right) forms. Fitting the pH-dependent (A) side chain $^{13}C^{\delta}$ and (B) backbone amide ^{15}N chemical shifts of Glu35, Glu78, Glu172 and the nonionizable reporter Gln7 (which primarily senses the ionization state of Glu78[10]) yields the indicated pK_a values (see Table 4). The pK_a value assigned to the predominant titration of a given residue is highlighted in bold coloring. These data were obtained from two-dimensional $^{1}H^{\gamma}(^{13}C^{\gamma})^{13}C^{\delta}$ and ^{15}N-HSQC spectra, respectively (not shown). A detailed summary of the fit pK_a values, associated chemical shift changes, and errors is provided in Supplemental Table S1.

requires that His35 acts as the hydrogen bond donor to Glu172, and thus must adopt the neutral $N^{\varepsilon 2}H$ tautomer both the apo enzyme and in the intermediate. Support for this conclusion is provided by long-range ^{15}N-HMBC spectra (Supplemental Figure S5). It is also noteworthy that in the structures of apo N35H-BcX, the side chain of Tyr174 shifts from a normally exposed, outward pointing position to stack over the imidazole ring of His35. This change, along with the concomitant repositioning of the adjacent exposed Gln175, could result from intermolecular interactions within the particular crystal lattice adopted by the mutant enzyme.

Reverse Protonation: Glu35 Elevates the pK_a of Glu172. The acid dissociation equilibria of the three Glu residues in N35E-BcX were also measured by NMR spectroscopy (Figure 7 and Supplemental Table S1). The $^{13}C^{\delta}$ chemical shifts of Glu78 in the apo enzyme followed a triphasic pH-titration with a fit pK_a value of 5.26 for the largest change. The assignment of the latter to ionization of Glu78 itself is supported by the similar pK_a values for the predominant titrations reported by the side chain $^{13}C^{\delta}$ of Gln7, as well as the amide ^{15}N of Glu78. The pK_a value of the catalytic nucleophile Glu78 corresponds approximately to the apparent pK_a value of 5.92 describing the basic limb of the pH-dependent k_{cat}/K_m profile of N35E-BcX, and thus is also indicative of a reverse protonation mechanism (Table 4).

On the basis of its pH-dependent $^{13}C^{\delta}$ chemical shifts, the pK_a value of Glu172 appears >8. Unfortunately, a reliable value could not be determined from titrations monitored with $^{1}H^{\gamma}(^{13}C^{\gamma})^{13}C^{\delta}$ spectra due to the weak Glu172 signal under alkaline conditions. This is likely due to $^{13}C^{\delta}$ exchange broadening that is often seen for Glu172 near its titration midpoint (e.g., Supplemental Figure S4). Accordingly, we also used ^{15}N-HSQC spectra to monitor the acid dissociation equilibria of N35E-BcX. As shown in Figure 7, we observed a major titration in the amide ^{15}N signal of Glu172 with a fit pK_a value of 8.08, as well as additional titrations with values at 5.16 (due to Glu78) and 3.47 (Glu35). Although the amide ^{15}N is a less reliable nucleus than the carboxyl $^{13}C^{\delta}$ for monitoring pH-titrations of glutamic acids due to its high sensitivity to pH-dependent conformational and electrostatic changes in a protein,[46] there are no other groups in BcX with pK_a values in this range, except perhaps the distal N-terminus. Furthermore, nuclei in both Glu78 and Glu35 also show minor titrations reporting this pK_a value. Thus, just as with the N35D variant,[12] Glu172 in apo N35E-BcX has an unusually high pK_a > 8 and alone cannot serve as the general acid.

The acidic limb of the pH-dependent k_{cat}/K_m profile of N35E-BcX follows an apparent pK_a value of 2.93. Since this differs significantly from those assigned to Glu78 and Glu172, we must conclude that it corresponds to Glu35, the only remaining carboxylic acid in the active site of the enzyme. Indeed, the $^{113}C^{\delta}$ of Glu35 follows a major titration with a pK_a value of 3.37. Therefore, Glu35 facilitates general acid catalysis, yet has a pK_a value lower than that of the nucleophile Glu78. This again indicates a reverse protonation mechanism for N35E-BcX. However, it is also noteworthy that the $^{13}C^{\delta}$ of

dx.doi.org/10.1021/bi400034m | *Biochemistry* 2013, 52, 3138−3156

Glu35 shows a second major pH-dependent chemical shift change with a fit pK_a value of 5.0. This likely reflects perturbations due to the ionization of Glu78, yet could also arise from a branched acid dissociation pathway. Unfortunately, we are unable to extract from NMR data alone the eight microscopic pK_a values describing the branched ionization equilibria of the three coupled Glu residues in this enzyme.

Upon formation of the trapped glycosyl-enzyme intermediate, 2FXb-modified Glu78 is neutral, and thus the electrostatic environments of Glu35 and Glu172 differ from those in the apo enzyme. The $^{13}C^{\delta}$ of Glu35 shows a strongly biphasic pH-titration with fit pK_a values of 3.44, assigned to itself, and 6.76 assigned to Glu172 (Figure 7 and Supplemental Table S1). This argument is supported by the minor $^{13}C^{\delta}$ and ^{15}N chemical shift changes of Glu172 near pH 3.5, and the larger ^{15}N titration with a fit pK_a value of 6.83. However, again it is difficult to confidently assign these macroscopic pK_a values to specific residues when the acid dissociation equilibria of the immediately adjacent Glu35 and Glu172 must be highly coupled. Thus, collectively, the two Glu residues show net deprotonation reactions with apparent pK_a values of ~3.4 and ~6.8 and serve as the general base for the deglycosylation of the covalently modified enzyme. This may at first seem surprising, but consideration of the pK_a values of the active site residues in the free enzyme after reaction reveals that the ultimate formal recipient of the proton is the catalytic nucleophile Glu78. All the Glu35−172 pair has to do is to shuttle the proton to Glu78 as the bond cleaves, which is not a challenging task with an activated substrate of this type.

The structures of apo and 2FXb-modified N35E-BcX were also determined by X-ray crystallography (Figure 5) and again found to be essentially superimposable upon those of the WT enzyme, including the skew-boat conformation of the covalently linked 2FXb moiety and a candidate nucleophilic water. In the case of the apo enzyme with two monomers in the asymmetric unit, Glu35 was observed in multiple conformations with O^{ε}-O^{ε} separations from Glu172 ranging between 3.5 Å to 6.1 Å. These distances are too long for a strong hydrogen bond, despite the possibility of such an interaction given that, under the crystallization conditions of pH 7 to 8, Glu35 should be ionized and Gly172 predominantly protonated. In the case of WT-BcX, Asn35 is 3.1 Å from Glu172 and at best only weakly hydrogen bonds. In the glycosyl-enzyme intermediate, only one conformation of Glu35 was observed in each monomer with O^{ε}-O^{ε} separations of 3.4 Å and 3.8 Å from Glu172. This stands in contrast to the N35D variant for which the Asp35-Glu172 separation drops significantly from 3.2 Å to 2.7 Å upon covalent-intermediate formation. The formation of this hydrogen bond in N35D-BcX, which is not seen with N35E-BcX, was postulated to substantially stabilize the transition state thus enhancing the efficiency of the enzyme and thereby offsetting the low population of its catalytically competent protonation state.[12] The lack of such a strong interaction in the N35E variant may lead to its reduced activity relative to the WT enzyme. This is also consistent with the observation that the pK_a values of the Asp35-Glu172 dicarboxylic acid pair in N35D-BcX are ~2.6 and >9, whereas in N35E-BcX they are less strongly perturbed.

DISCUSSION

In this study, we have examined a variety of strategies aimed at manipulating the pK_a values of the nucleophile and general acid/base catalytic groups in BcX, and thereby altering the pH_{opt} of this enzyme. These approaches included changing the global charge of BcX by random chemical modification, introducing altered charged residues at numerous positions flanking the active site, and specifically targeting the general acid Glu172 and its neighboring Asn35. The mutant proteins were characterized kinetically with a defined substrate to yield the apparent pK_a values governing their pH-dependent activity, as well as by NMR spectroscopy to provide site-specific pK_a values for residues 35, 78, and 172, and by X-ray crystallography to obtain high resolution structural information. Collectively, these data provide many interesting and often nonintuitive insights into the factors that contribute to the pH-dependent activity of BcX, and by inference, GH-11 xylanases in general. These data also illustrate the challenges in interpreting enzyme pH-dependent kinetic parameters, as articulated clearly in a seminal review by Knowles.[47]

BcX pH_{opt} Is Independent of its Global Charge. Initially, we tested the hypothesis that altering the global charge of BcX could alter the electrostatic environment of its catalytic residues and thereby perturb their pK_a values. However, randomly succinylating the protein at 4−8 positions did not significantly perturb its pH-dependent activity, despite the reduction in its predicted pI value from ~9 to as low as ~4.5. Therefore, there is no simple, direct correlation between the pH_{opt} of BcX and its global charge. In many respects, this result is not unexpected given that the most readily succinylated amino and phenyl groups are likely solvent exposed, and that the five lysines and the amino terminus are all distal from the active site of BcX.

The CAZy database[7] currently lists over 650 GH-11 xylanases, many of which are from extremophile organisms and exhibit a remarkable range of pH-dependent properties.[9] Accordingly, there have been numerous studies aimed at defining the factors that establish their adaptation for activity under unusually low or high pH conditions. Consistent with effects of succinylation on BcX, there is no clear correlation between the predicted pI value of a GH-11 xylanase and its reported pH_{opt} for activity (e.g., Table 3 of Sapag et al.[5] and Table 4 of Paes et al.[9]). For a subset of characterized family members, it has been suggested that pH_{opt} decreases with increasing (Asp + Glu)/(Arg + Lys) ratio.[48] However, the opposite trend has been identified for GH-10 xylanases,[49] and indeed one would expect that the increased negative electrostatic potential from additional aspartates and glutamates should elevate the pK_a values of the catalytic residues and thereby increase pH_{opt}. It is possible that these correlations relate to additional factors, such as the pH-dependent folding and stability of the xylanases under the environmental conditions experienced by their host organisms.[50] However, no generally applicable paradigm exists.

The effects of surface charge on pH-dependent activity of an enzyme are likely dependent upon several specific, rather than global, factors relating to the precise structural and electrostatic (dielectric) environment of its catalytic residues. For example, succinylation of 14 lysines in chymotrypsin only raised the apparent pK_a value of an active site residue by 1 log unit,[51] whereas an effect of similar magnitude resulted from as few as four charge-changing mutations of surface residues in subtilisin.[52] Engineering surface charges can also significantly alter the pK_a values of an ionizable group buried within the low dielectric interior of a protein.[53] Indeed, the pH-dependent activity of a cellulase has been modulated by mutation of

dx.doi.org/10.1021/bi400034m | Biochemistry 2013, 52, 3138−3156

surface residues,[54] and it is likely that similar specific examples also hold for GH-11 xylanases.

Second Shell Mutations can Alter the pH-Dependent Activity of BcX. Mutation of residues directly contacting Glu78 and Glu172 generally impaired the catalytic activity of BcX,[11] whereas succinylation of distal, exposed residues had little effect. Therefore, we reasoned that changing the charges of loosely defined "second shell" residues might alter the electrostatic environments of the active site without adversely perturbing its structure. Indeed, numerous studies, guided by sequence comparisons, have identified such residues flanking the active sites of GH-11 xylanases that potentially contribute to their particular pH-dependent activity.[5,9] To test this hypothesis, we introduced single charge-changing mutations at 14 sites in BcX. Most of these mutations involved the addition of an Asp or Glu side chain, with the expectation that these negatively charged carboxylates might increase the pK_a values of Glu78 and Glu172, and thereby raise the pH_{opt} of BcX.

In many cases, including N63D, Y88D, T110D, T111D, R112G, T126D, Y174D, the mutations had little effect ($|\Delta pK_a| < 0.3$) on the pH-dependent activity profile of BcX. Three actually led to small increases (1.2−3 fold) in activity for reasons that are not immediately obvious. Of the 14 sites considered, these 7 are among the most solvent exposed and distal (7−14 Å) from Glu78 and Glu172. However, the Q7E, R73A, and G92D mutations led to more substantial pK_a changes (ΔpK_a = −0.5 to −0.9 for Glu78) and modest reductions in activity, yet each of these sites is even further from the catalytic glutamic acids. The largest effects resulted from the Q7K, T67D, A115E, R112E, S117D, and Q127H mutations (ΔpK_a = −0.8 to −1.6 for Glu78; ΔpK_a = −0.2 to +0.7 for Glu172), but in each case, the relative activity of BcX also decreased by at least 7 fold. Gln127 is a first-shell residue that hydrogen bonds to Glu78, whereas Gln7 is partially buried at the edge of the active site, Thr67 is fully buried within the active site, and Ala115 and Ser117 are partially buried within the adjacent "thumb" region. The changes in the pK_a values assigned to Glu78 and Glu172 may therefore result from stronger electrostatic effects due to introducing charged residues within the low dielectric interior of BcX, and the reduction in activity due to possible structural perturbations. Alternatively, with a substantially reduced pK_a value, even though more of Glu78 will be deprotonated, it will also be a weaker nucleophile; likewise with an increased pK_a value, Glu172 becomes a weaker general acid.

Perhaps the most unexpected result is that the introduction of both negatively (Asp, Glu) and positively (Lys, His) charged groups, or the removal of an Arg, all led to a *reduction* in the pH_{opt} of BcX. The shifts in the pH-dependent activity profiles of these mutants result primarily from a reduction in the acidic limb pK_a value that is attributed to Glu78. This is understandable in the cases of the Q127H and Q7K mutants, where the introduced side chain is almost certainly positively charged near the pH_{opt} of the mutant and thus would favor deprotonation of Glu78. However, mutations to Asp or Glu should either have little effect on Glu78 or should increase its pK_a value (i.e., if the "intrinsic" pK_a value of the introduced residue is greater than or less than that of Glu78, then with increasing sample pH, Glu78 will predominantly deprotonate in the context of the neutral or charged mutated residue, respectively). The observation that the pK_a values assigned to Glu78 actually decreased indicates that the effects of the mutations are more complex than naively expected from a simple charge change, and may also involve structural perturbations, including altered solvation and local dielectric environment.

Collectively, these data indicate that "second shell" residues help establish the pH-dependent activity of BcX. However, sites where mutations had the largest effects also tended to compromise the overall catalytic activity of the enzyme. Thus, it is plausible that the selective combination of many relatively nonperturbing charge-change mutations may collectively lead to a significant shift in the pH_{opt} of BcX without net loss of activity.[55] Indeed, it is likely that the pH-dependent properties of GH-11 xylanases, including those from extremophiles, are established by the collective effect of many amino acids. One exception to this statement is position 35, as discussed below.

Histidine Can Serve as the General Acid/Base in BcX. GH-11 xylanases invariably exploit Glu residues as both the nucleophile and general acid/base,[5,9] and even the conservative substitution of an Asp at either position leads to a dramatic reduction in activity.[56,57] Remarkably, the E127H mutant retained ∼8% activity toward a xylobioside substrate (ONPX2) and exhibited a dramatically shifted pH_{opt} of 4.67. Preliminary measurements confirmed that the enzyme was also active against birchwood xylan. The kinetically determined pK_a values of 3.78 and 5.56 governing the acidic and basic limbs of its pH-dependent k_{cat}/K_m activity profile approximately matched those determined by NMR spectroscopy for Glu78 (pK_a = 3.39) and His172 (pK_a = 5.22), respectively. Therefore, as summarized in Figure 8, E172H-BcX follows a normal protonation mechanism with Glu78 predominantly ionized at its pH_{opt} to serve as a nucleophile and His172 protonated to function as a general acid. These kinetic roles are confirmed by X-ray crystallographic studies of E172H-BcX, which revealed that its structure superimposes closely upon that of WT-BcX and that Glu78 becomes covalently modified in the glycosyl-enzyme intermediate formed by reaction with DNP2FXb. Furthermore, similar to WT-BcX,[10] the NMR spectroscopically measured pK_a value of His172 in this intermediate dropped to ∼3, thus enabling it to serve as a general base during the deglycosylation step. However, in contrast to the well-ordered side chain of Glu172 in WT-BcX, multiple conformations were observed for the imidazole ring of the non-naturally occurring His172, both directly by X-ray crystallography and indirectly by NMR spectroscopy.

Glu78 and His172 are strongly electrostatically coupled due to their separation of only ∼6 Å across the active site of E172H-BcX. When Glu78 is negatively charged, the pK_a value of His172 is 5.22, whereas it drops dramatically by 2.4 log units when Glu78 is neutralized upon covalent modification in the trapped glycosyl enzyme intermediate. This electrostatic coupling is likely key to the pK_a cycling of His172, enabling it to serve as a general acid during the glycosylation step and a general base during deglycosylation. Although elevated by favorable interactions with Glu78, the pK_a value of 5.22 for His172 is still lower than that of 6.5 for a histidine in a random-coil polypeptide,[42] and therefore its neutral form is favored within the folded state of BcX. This is likely due to its partially buried environment and lack of suitable hydrogen-bonding partners, and reflects the fact that GH-11 xylanases have not evolved to accommodate a catalytic histidine at this site.

The finding that histidine can nevertheless serve as a general acid/base is most intriguing. Despite earlier expectations that glycoside hydrolases would use such residues (largely based on

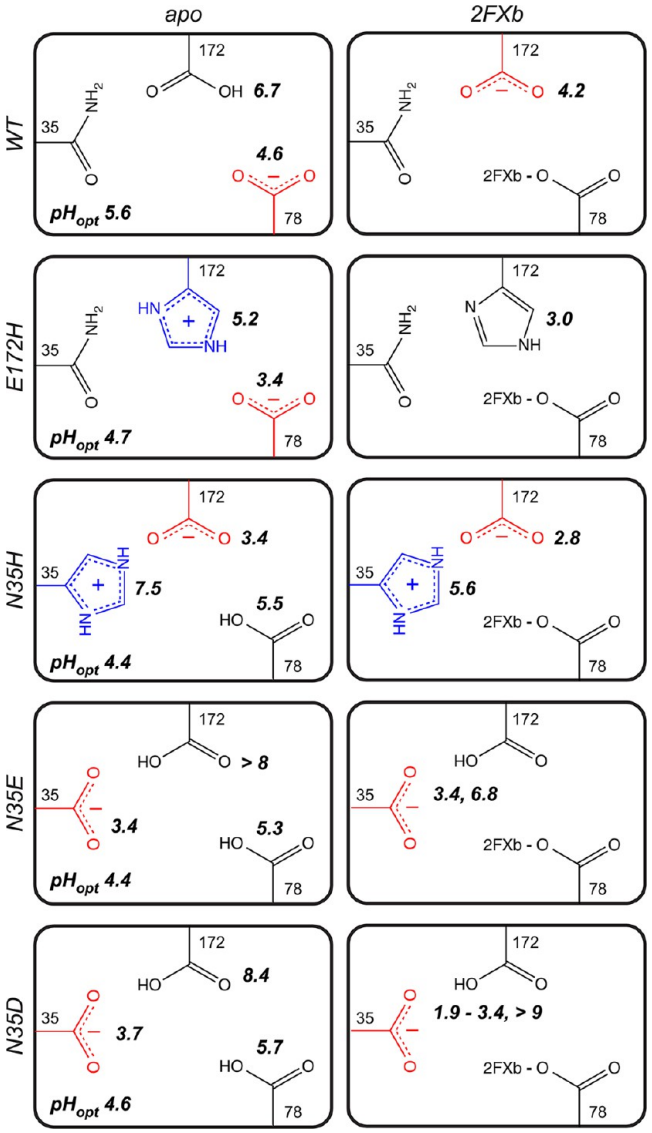

Figure 8. Summary of the major NMR-spectroscopically determined pK_a values and predominant ionization states of residues 35, 78, and 172 at the pH_{opt} of the indicated BcX variants in their apo and 2FXb glycosyl-enzyme intermediate forms (red, negative; blue, positive; black, neutral). The rounded-off data are taken from Table 4 and Supplemental Table S1. For His35 in both forms of N35H-BcX and His172 in modified E172H-BcX, the average pK_a values from the $^1H^{\varepsilon 1}$- and $^{13}C^{\varepsilon 1}$-monitored titrations are indicated. In the cases of 2FXb-modified N35E- and N35D-BcX, Glu/Asp35 and Glu172 are strongly coupled and thus it is difficult to assign to the measured pK_a to values specific residues.

crude and unverified inactivation studies with diethylpyrocarbonate or Rose Bengal), the only example actually demonstrated to date is the GH-3 *Bacillus subtilis* N-acetylglucosaminidase.[58] It this specific case, it was argued that the reason for a general acid/base histidine may be to minimize unfavorable active site interactions with the charged peptidoglycan substrate. Interestingly some glycosyltransferases, especially sialyltransferases, also use histidine in this catalytic role, possibly to avoid repulsive electrostatic interactions with charged substrates in their active sites.[59] Indeed it is plausible that the choice of carboxylic acids as the preferred general acid/base residues in glycoside hydrolases such as BcX is partially the result of selection against enzyme forms that might unproductively cleave sugar 1-phosphates or their nucleotide versions.

Reverse Protonation: Both N35H and N35E Reduce the pH_{opt} of BcX. It is well established that the pH_{opt} of GH-11 xylanases is determined in large part by the nature of one key residue neighboring the general acid/base. Specifically, an Asp is present in those enzymes with a relatively low pH_{opt}, whereas an Asn is found in those most active under more neutral or alkaline conditions.[9] Previously, we characterized in great detail the N35D mutant of BcX, demonstrating that it indeed has a reduced pH_{opt} relative to the WT enzyme and follows a reverse protonation mechanism in which the pK_a of the general acid (effectively Asp35) is lower than that of the nucleophile Glu78.[12] To test the generality of this phenomenon, we generated mutants with either a His and Glu at position 35. Neither of these residues is found with any appreciable frequency at this position in naturally occurring GH-11 xylanases.[9]

Both N35H- and N35E-BcX also exhibited significantly reduced pH_{opt} values of ∼4.4. Similar to the N35D variant, introduction of a histidine at position 35 led to a modest 1.2 fold increase in activity. In contrast, the activity of the N35E mutant was reduced by ∼6 fold. Regardless, for both mutants, NMR spectroscopic measurements revealed that the pK_a value of the nucleophile Glu78 corresponded to the basic limb of the pH-dependent activity profile, whereas that of either Glu172 in the N35H mutant or Glu35 in the N35E mutant corresponded to the acidic limb (Figure 8). Importantly, X-ray crystallographic studies confirmed that the mutants retain the structure of WT-BcX, and that Glu78 is indeed the nucleophile. In each case, this is diagnostic of a reverse protonation mechanism in which the pK_a value of the nucleophile is higher than that of the general acid, and therefore, at its pH_{opt}, only a small fraction of the enzyme is in a catalytically competent ionization state with the nucleophile deprotonated and the general acid protonated.[13] Parenthetically, it may not seem intuitive that the kinetically determined pK_a values from the pH-dependence of k_{cat}/K_m would match the site-specific pK_a values measured by NMR spectroscopy for a reverse protonation mechanism. However, it is important to recognize that the major population of enzyme with the nucleophile protonated and the general acid deprotonated is in a *pH-independent* equilibrium with the minor catalytically competent population having the opposite tautomeric configuration.

As with many of the "second-shell" mutants discussed above, it is striking that the introduction of either a positively or negatively charged residue at position 35 results in a reduction of the pH_{opt} of BcX. In the case of N35H-BcX, this is somewhat easier to understand as His35, with a pK_a value of 7.48, reduces the pK_a value of the adjacent Glu172 to 3.39 through favorable electrostatic interactions. Although only present with a low population at the pH_{opt} of N35H-BcX, Glu172 is effectively a stronger general acid and therefore the net activity of the enzyme is comparable to that of WT-BcX. In the glycosyl-enzyme intermediate, the pK_a value of Glu172 drops by ∼0.5 log units to ∼3, and the residue functions as a general base. Given that the "intrinsic" pK_a value of Glu172 is lower than that of Glu78, this change is not likely a result of neutralization of the nucleophile, but rather might reflect changes in the local environment and solvation of Glu172 due to the 2FXb moiety in the active site.

As with the initial N35D mutant, the effects of Glu35 on the activity of BcX are more difficult to understand. In particular, all

dx.doi.org/10.1021/bi400034m | *Biochemistry* 2013, 52, 3138−3156

three Glu residues in the active site of N35E-BcX are electrostatically coupled and yield multiphasic titration curves. Thus assigning pK_a values to specific residues is somewhat ambiguous as each titration curve reflects an averaged or macroscopic behavior of the entire protein. With this in mind, electrostatic repulsion between Glu35 and Glu172 elevates the pK_a value of Glu172 to >8 and renders it too weak a general acid to contribute to catalysis. Therefore Glu35 appears to set the acid limb of the pH-dependent activity profile of N35E-BcX, and as such must serve as the general acid. Given the stereochemical constraints of proton transfer and the close juxtapositioning of Glu35 and Glu172, it is reasonable to consider the two residues as a coupled dicarboxylic acid pair, from which the loss of the one proton facilitates aglycone departure. In the case of N35D-BcX, Asp35 and Glu172 form a closely hydrogen-bonded pair in the resulting glycosyl enzyme intermediate. This has been proposed to compensate for the low population of the catalytically competent ionization state of the protein by enhancing its catalytic efficiency. Such a strong interaction is not observed in the structures of the apo and 2FXb-modified forms of N35E-BcX, and this might account for its reduced activity.

In conclusion, by combining kinetic studies with pK_a measurements by NMR spectroscopy and structural analyses by X-ray crystallography, we are able to provide detailed explanations for the altered pH-dependent activities of several BcX variants. These results both define strategies to engineer the pH_{opt} of xylanases for biotechnological applications and provide a rich database for developing improved algorithms to accurately predict electrostatic interactions within the complex environment of a protein.

■ ASSOCIATED CONTENT

Supporting Information

One table summarizing the fitting of NMR-monitored titration curves and five figures summarizing additional NMR spectra. This material is available free of charge via the Internet at http://pubs.acs.org.

■ AUTHOR INFORMATION

Corresponding Author

*Address: Department of Biochemistry and Molecular Biology, Life Sciences Centre, 2350 Health Sciences Mall, University of British Columbia, Vancouver, BC, Canada, V6T 1Z3. Phone: 001-604-822-3341. Fax: 001-604-822-5227. E-mail: mcintosh@chem.ubc.ca.

Funding

This research was funded by the Natural Sciences and Engineering Research Council of Canada (NSERC) to L.P.M. and S.G.W. Instrument support was provided by the Canadian Institutes for Health Research, the Canadian Foundation for Innovation (CFI), the British Columbia Knowledge Development Fund (BCKDF), the UBC Blusson Fund, and the Michael Smith Foundation for Health Research (MSFHR).

Notes

The authors declare no competing financial interest.

■ ACKNOWLEDGMENTS

We thank David Waugh for kindly providing several bacterial strains, and Frank Löhr and Lewis Kay for initial NMR pulse sequences. M.L.L. acknowledges an Erwin Schrödinger Fellowship from the Austrian Science Fund, I.D. acknowledges postdoctoral support from the MSFHR, and S.G.W. thanks the Canada Research Chairs program for salary support.

■ ABBREVIATIONS USED

BcX, *Bacillus circulans* xylanase; DNP2FXb, 2,4-dinitrophenyl 2-deoxy-2-fluoro-β-xylobioside; ESI-MS, electrospray ionization mass spectrometry; 2FXb-BcX, 2-deoxy-2-fluoro-β-xylobiosyl-BcX; ONPX2, 2′-nitrophenyl β-xylobioside

■ REFERENCES

(1) Zechel, D. L., and Withers, S. G. (2000) Glycosidase mechanisms: anatomy of a finely tuned catalyst. *Acc. Chem. Res. 33*, 11−18.

(2) Rye, C. S., and Withers, S. G. (2000) Glycosidase mechanisms. *Curr. Opin. Chem. Biol. 4*, 573−580.

(3) Vocadlo, D. J., and Davies, G. J. (2008) Mechanistic insights into glycosidase chemistry. *Curr. Opin. Chem. Biol. 12*, 539−555.

(4) Davies, G. J., Planas, A., and Rovira, C. (2012) Conformational analyses of the reaction coordinate of glycosidases. *Acc. Chem. Res. 45*, 308−316.

(5) Sapag, A., Wouters, J., Lambert, C., de Ioannes, P., Eyzaguirre, J., and Depiereux, E. (2002) The endoxylanases from family 11: computer analysis of protein sequences reveals important structural and phylogenetic relationships. *J. Biotechnol. 95*, 109−131.

(6) Collins, T., Gerday, C., and Feller, G. (2005) Xylanases, xylanase families and extremophilic xylanases. *FEMS Micro. Rev. 29*, 3−23.

(7) Cantarel, B. L., Coutinho, P. M., Rancurel, C., Bernard, T., Lombard, V., and Henrissat, B. (2009) The Carbohydrate-Active EnZymes database (CAZy): an expert resource for Glycogenomics. *Nucleic Acids Res. 37*, D233−238.

(8) Pollet, A., Delcour, J. A., and Courtin, C. M. (2010) Structural determinants of the substrate specificities of xylanases from different glycoside hydrolase families. *Crit. Rev. Biotechnol. 30*, 176−191.

(9) Paes, G., Berrin, J. G., and Beaugrand, J. (2012) GH11 xylanases: Structure/function/properties relationships and applications. *Biotech. Adv. 30*, 564−592.

(10) McIntosh, L. P., Hand, G., Johnson, P. E., Joshi, M. D., Korner, M., Plesniak, L. A., Ziser, L., Wakarchuk, W. W., and Withers, S. G. (1996) The pK_a of the general acid/base carboxyl group of a glycosidase cycles during catalysis: A ^{13}C-NMR study of *Bacillus circulans* xylanase. *Biochemistry 35*, 9958−9966.

(11) Joshi, M. D., Sidhu, G., Nielsen, J. E., Brayer, G. D., Withers, S. G., and McIntosh, L. P. (2001) Dissecting the electrostatic interactions and pH-dependent activity of a family 11 glycosidase. *Biochemistry 40*, 10115−10139.

(12) Joshi, M. D., Sidhu, G., Pot, I., Brayer, G. D., Withers, S. G., and McIntosh, L. P. (2000) Hydrogen bonding and catalysis: A novel explanation for how a single amino acid substitution can change the pH optimum of a glycosidase. *J. Mol. Biol. 299*, 255−279.

(13) Mock, W. L. (1992) Theory of enzymatic reverse-protonation catalysis. *Bioorg. Chem. 20*, 377−381.

(14) Sung, W. L., Luk, C. K., Zahab, D. M., and Wakarchuk, W. (1993) Overexpression and purification of the *Bacillus subtilis* and *Bacillus circulans* xylanases in *Escherichia coli*. *Prot. Express. Purif. 4*, 200−216.

(15) Kunkel, T. A., Roberts, J. D., and Zakour, R. A. (1987) Rapid and efficient site-specific mutagenesis without phenotypic selection. *Meth. Enzymol. 154*, 367−382.

(16) Wakarchuk, W. W., Campbell, R. L., Sung, W. L., Davoodi, J., and Yaguchi, M. (1994) Mutational and crystallographic analyses of the active site residues of the *Bacillus circulans* xylanase. *Protein Sci. 3*, 467−475.

(17) LeMaster, D. M., and Richards, F. M. (1988) NMR sequential assignment of *Escherichia coli* thioredoxin utilizing random fractional deuteriation. *Biochemistry 27*, 142−150.

(18) Waugh, D. S. (1996) Genetic tools for selective labeling of proteins with alpha-^{15}N-amino acids. J. *Biomol. NMR 8*, 184−192.

(19) Muchmore, D. C., McIntosh, L. P., Russell, C. B., Anderson, D. E., and Dahlquist, F. W. (1989) Expression and nitrogen-15 labeling of proteins for proton and nitrogen-15 nuclear magnetic resonance. *Methods Enzymol. 177*, 44−73.
(20) Sidhu, G., Withers, S. G., Nguyen, N. T., McIntosh, L. P., Ziser, L., and Brayer, G. D. (1999) Sugar ring distortion in the glycosyl-enzyme intermediate of a family G/11 xylanase. *Biochemistry 38*, 5346−5354.
(21) Delaglio, F., Grzesiek, S., Vuister, G. W., Zhu, G., Pfeifer, J., and Bax, A. (1995) NMRPipe: a multidimensional spectral processing system based on UNIX pipes. *J Biomol. NMR 6*, 277−293.
(22) Goddard, T. D., and Kneeler, D. G. (1999) *Sparky 3*, University of California, San Francisco.
(23) Pelton, J. G., Torchia, D. A., Meadow, N. D., and Roseman, S. (1993) Tautomeric states of the active-site histidines of phosphorylated and unphosphorylated III(Glc), a signal-transducing protein from *Escherichia coli*, using 2-dimensional heteronuclear NMR techniques. *Protein Sci. 2*, 543−558.
(24) Mulder, F. A. A., Spronk, C. A. E. M., Slijper, M., Kaptein, R., and Boelens, R. (1996) Improved HSQC experiments for the observation of exchange broadened signals. *J. Biomol. NMR 8*, 223−228.
(25) Schubert, M., Poon, D. K. Y., Wicki, J., Tarling, C. A., Kwan, E. M., Nielsen, J. E., Withers, S. G., and McIntosh, L. P. (2007) Probing electrostatic interactions along the reaction pathway of a glycoside hydrolase: Histidine characterization by NMR spectroscopy. *Biochemistry 46*, 7383−7395.
(26) Löhr, F., and Rüterjans, H. (1996) Novel pulse sequences for the resonance assignment of aromatic side chains in ^{13}C-labeled proteins. *J. Magn. Reson. Ser. B 112*, 259−268.
(27) Kay, L. (1993) Pulsed-field gradient-enhanced three-dimensional NMR experiment for correlating $^{13}C\alpha/\beta$, $^{13}C'$, and $^{1}H\alpha$ chemical shifts in uniformly ^{13}C labelled proteins dissolved in H_20. *J. Am. Chem. Soc. 115*, 2055−2057.
(28) Oda, Y., Yamazaki, T., Nagayama, K., Kanaya, S., Kuroda, Y., and Nakamura, H. (1994) Individual ionization constants of all the carboxyl groups in Ribonuclease HI from *Escherichia coli* determined by NMR. *Biochemistry 33*, 5275−5284.
(29) Plesniak, L. A., Connelly, G. P., Wakarchuk, W. W., and McIntosh, L. P. (1996) Characterization of a buried neutral histidine residue in *Bacillus circulans* xylanase: NMR assignments, pH titration, and hydrogen exchange. *Protein Sci. 5*, 2319−2328.
(30) Connelly, G. P., and McIntosh, L. P. (1998) Characterization of a buried neutral histidine in *Bacillus circulans* xylanase: internal dynamics and interaction with a bound water molecule. *Biochemistry 37*, 1810−1818.
(31) Sattler, M., Schleucher, J., and Griesinger, C. (1999) Heteronuclear multidimensional NMR experiments for the structure determination of proteins in solution employing pulsed field gradients. *Prog. Nucl. Magn. Reson. Spectrosc. 34*, 93−158.
(32) McIntosh, L. P., Naito, D., Baturin, S. J., Okon, M., Joshi, M. D., and Nielsen, J. E. (2011) Dissecting electrostatic interactions in *Bacillus circulans* xylanase through NMR-monitored pH titrations. *J. Biomol. NMR 51*, 5−19.
(33) Otwinowski, Z., and Minor, W. (1997) Processing of X-ray diffraction data collected in oscillation mode. *Macromol. Cryst. Part A 276*, 307−326.
(34) Mccoy, A. J., Grosse-Kunstleve, R. W., Adams, P. D., Winn, M. D., Storoni, L. C., and Read, R. J. (2007) Phaser crystallographic software. *J. Appl. Crystallogr. 40*, 658−674.
(35) Brunger, A. T., Adams, P. D., Clore, G. M., DeLano, W. L., Gros, P., Grosse-Kunstleve, R. W., Jiang, J. S., Kuszewski, J., Nilges, M., Pannu, N. S., Read, R. J., Rice, L. M., Simonson, T., and Warren, G. L. (1998) Crystallography & NMR system: A new software suite for macromolecular structure determination. *Acta Crystallogr., Sect. D: Biol. Crystallogr. 54*, 905−921.
(36) Murshudov, G. N., Vagin, A. A., and Dodson, E. J. (1997) Refinement of macromolecular structures by the maximum-likelihood method. *Acta Crystallogr., Sect. D: Biol. Crystallogr. 53*, 240−255.
(37) Emsley, P., Lohkamp, B., Scott, W. G., and Cowtan, K. (2010) Features and development of Coot. *Acta Crystallogr., Sect. D: Biol. Crystallogr. 66*, 486−501.
(38) Baturin, S. J., Okon, M., and McIntosh, L. P. (2011) Structure, dynamics, and ionization equilibria of the tyrosine residues in *Bacillus circulans* xylanase. *J. Biomol. NMR 51*, 379−394.
(39) Means, G. E., and Feeney, R. E. (1971) *Chemical Modification of Proteins*, Holden-Day, San Francisco, CA.
(40) Haynes, W. M. (2011) *CRC Handbook of Chemistry and Physics* (Haynes, W. M., Ed.), Chapman and Hall, Boca Raton, FL.
(41) Joshi, M. D., Hedberg, A., and McIntosh, L. P. (1997) Complete measurement of the pK_a values of the carboxyl and imidazole groups in *Bacillus circulans* xylanase. *Protein Sci. 6*, 2667−2670.
(42) Grimsley, G. R., Scholtz, J. M., and Pace, C. N. (2009) A summary of the measured pK values of the ionizable groups in folded proteins. *Protein Sci. 18*, 247−251.
(43) Willard, L., Ranjan, A., Zhang, H., Monzavi, H., Boyko, R. F., Sykes, B. D., and Wishart, D. S. (2003) VADAR: a web server for quantitative evaluation of protein structure quality. *Nucleic Acids Res. 31*, 3316−3319.
(44) Miao, S., Ziser, L., Aebersold, R., and Withers, S. G. (1994) Identification of glutamic acid 78 as the active site nucleophile in *Bacillus subtilis* xylanase using electrospray tandem mass spectrometry. *Biochemistry 33*, 7027−7032.
(45) Sabini, E., Wilson, K. S., Danielsen, S., Schulein, M., and Davies, G. J. (2001) Oligosaccharide binding to family 11 xylanases: both covalent intermediate and mutant product complexes display ^{2,5}B conformations at the active centre. *Acta Crystallogr., Sect. D: Biol. Crystallogr. 57*, 1344−1347.
(46) Webb, H., Tynan-Connolly, B. M., Lee, G. M., Farrell, D., O'Meara, F., Sondergaard, C. R., Teilum, K., Hewage, C., McIntosh, L. P., and Nielsen, J. E. (2011) Remeasuring HEWL pK_a values by NMR spectroscopy: Methods, analysis, accuracy, and implications for theoretical pK_a, calculations. *Proteins 79*, 685−702.
(47) Knowles, J. R. (1976) Intrinsic pKa values of functional groups in enzymes - Improper deductions from pH-dependence of steady-state parameters. *CRC Crit. Rev. Biochem. 4*, 165−173.
(48) Michaux, C., Pouyez, J., Mayard, A., Vandurm, P., Housen, I., and Wouters, J. (2010) Structural insights into the acidophilic pH adaptation of a novel endo-1,4-beta-xylanase from *Scytalidium acidophilum*. *Biochimie 92*, 1407−1415.
(49) Mamo, G., Thunnissen, M., Hatti-Kaul, R., and Mattiasson, B. (2009) An alkaline active xylanase: insights into mechanisms of high pH catalytic adaptation. *Biochimie 91*, 1187−1196.
(50) Poon, D. K. Y., Ludwiczek, M. L., Schubert, M., Kwan, E. M., Withers, S. G., and McIntosh, L. P. (2007) NMR spectroscopic characterization of a beta-(1,4)-glycosidase along its reaction pathway: Stabilization upon formation of the glycosyl-enzyme intermediate. *Biochemistry 46*, 1759−1770.
(51) Valenzuela, P., and Bender, M. L. (1971) Kinetic properties of succinylated and ethylenediamine-amidated -chymotrypsins. *Biochem. Biophys. Acta 250*, 538−548.
(52) Russell, A. J., and Fersht, A. R. (1987) Rational modification of enzyme catalysis by engineering surface charge. *Nature 328*, 496−500.
(53) Pey, A. L., Rodriguez-Larrea, D., Gavira, J. A., Garcia-Moreno, B., and Sanchez-Ruiz, J. M. (2010) Modulation of buried ionizable groups in proteins with engineered surface charge. *J. Am. Chem. Soc. 132*, 1218−1219.
(54) Cockburn, D. W., and Clarke, A. J. (2011) Modulating the pH-activity profile of cellulase A from *Cellulomonas fimi* by replacement of surface residues. *Protein Eng. Des. Select. 24*, 429−437.
(55) Tynan-Connolly, B. M., and Nielsen, J. E. (2007) Redesigning protein pKa values. *Protein Sci. 16*, 239−249.
(56) Lawson, S. L., Wakarchuk, W. W., and Withers, S. G. (1996) Effects of both shortening and lengthening the active site nucleophile of *Bacillus circulans* xylanase on catalytic activity. *Biochemistry 35*, 10110−10118.

(57) Lawson, S. L., Wakarchuk, W. W., and Withers, S. G. (1997) Positioning the acid/base catalyst in a glycosidase: Studies with *Bacillus circulans* xylanase. *Biochemistry 36*, 2257−2265.
(58) Litzinger, S., Fischer, S., Polzer, P., Diederichs, K., Welte, W., and Mayer, C. (2010) Structural and kinetic analysis of *Bacillus subtilis* N-acetylglucosaminidase reveals a unique Asp-His dyad mechanism. *J. Biol. Chem. 285*, 35675−35684.
(59) Chan, P. H., Lairson, L. L., Lee, H. J., Wakarchuk, W. W., Strynadka, N. C., Withers, S. G., and McIntosh, L. P. (2009) NMR spectroscopic characterization of the sialyltransferase CstII from *Campylobacter jejuni*: histidine 188 is the general base. *Biochemistry 48*, 11220−11230.
(60) DeLano, W. L., and Lam, J. W. (2005) PyMOL: A communications tool for computational models. *Abs. Paper Am. Chem. Soc. 230*, U1371−U1372.